

Review

The Role of the Metabolism of Zinc and Manganese Ions in Human Cancerogenesis

Julian Markovich Rozenberg ^{1,*}, Margarita Kamynina ², Maksim Sorokin ^{1,2}, Marianna Zolotovskaia ^{1,3}, Elena Koroleva ¹, Kristina Kremenchutckaya ¹, Alexander Gudkov ², Anton Buzdin ^{1,2,3,4,5} and Nicolas Borisov ^{1,3}

- ¹ Moscow Institute of Physics and Technology, National Research University, 141700 Moscow, Russia; sorokin@oncobox.com (M.S.); zolotovskaia.ma@mipt.ru (M.Z.); koroleva@oncobox.com (E.K.); krem-kristina@mail.ru (K.K.); buzdin@oncobox.com (A.B.); borisov@oncobox.com (N.B.)
- ² Group of Experimental Biotherapy and Diagnostic, Institute for Regenerative Medicine, I.M. Sechenov First Moscow State Medical University, 119991 Moscow, Russia; margaret.kamynina@gmail.com (M.K.); dr.gudkov@gmail.com (A.G.)
- ³ OmicsWay Corporation, Walnut, CA 91789, USA
- ⁴ Shemyakin-Ovchinnikov Institute of Bioorganic Chemistry, Russian Academy of Sciences, 117997 Moscow, Russia
- ⁵ Oncobox Ltd., 121205 Moscow, Russia
- * Correspondence: rozenbej@gmail.com

Abstract: Metal ion homeostasis is fundamental for life. Specifically, transition metals iron, manganese and zinc play a pivotal role in mitochondrial metabolism and energy generation, anti-oxidation defense, transcriptional regulation and the immune response. The misregulation of expression or mutations in ion carriers and the corresponding changes in Mn^{2+} and Zn^{2+} levels suggest that these ions play a pivotal role in cancer progression. Moreover, coordinated changes in Mn^{2+} and Zn^{2+} ion carriers have been detected, suggesting that particular mechanisms influenced by both ions might be required for the growth of cancer cells, metastasis and immune evasion. Here, we present a review of zinc and manganese pathophysiology suggesting that these ions might cooperatively regulate cancerogenesis. Zn and Mn effects converge on mitochondria-induced apoptosis, transcriptional regulation and the cGAS-STING signaling pathway, mediating the immune response. Both Zn and Mn influence cancer progression and impact treatment efficacy in animal models and clinical trials. We predict that novel strategies targeting the regulation of both Zn and Mn in cancer will complement current therapeutic strategies.

Keywords: zinc; manganese; transitional elements; microelements; cancer; tumorigenesis; molecular pathways; cell growth signaling



Citation: Rozenberg, J.M.; Kamynina, M.; Sorokin, M.; Zolotovskaia, M.; Koroleva, E.; Kremenchutckaya, K.; Gudkov, A.; Buzdin, A.; Borisov, N. The Role of the Metabolism of Zinc and Manganese Ions in Human Cancerogenesis. *Biomedicines* **2022**, *10*, 1072. <https://doi.org/10.3390/biomedicines10051072>

Academic Editors: Demin Cai and Chengfei Liu

Received: 15 April 2022

Accepted: 3 May 2022

Published: 5 May 2022

Publisher's Note: MDPI stays neutral with regard to jurisdictional claims in published maps and institutional affiliations.



Copyright: © 2022 by the authors. Licensee MDPI, Basel, Switzerland. This article is an open access article distributed under the terms and conditions of the Creative Commons Attribution (CC BY) license (<https://creativecommons.org/licenses/by/4.0/>).

1. Introduction

Transitional metals, including iron, manganese and zinc, are widely employed in numerous biochemical reactions. According to the periodic table, Mn is located nearby Fe, with a similar size of atoms and electron configuration of outer orbitals (Mn: 127 pm, 3d⁵ 4s² and Fe: 128 pm, 3d⁶ 4s²), thus suggesting similar, but not identical, chemical properties. In the biologically relevant 3+ ionization form, ionic radii and electron configurations are also similar: Mn^{3+} : 72 pm 3d⁴ and Fe^{3+} : 69 pm, 3d⁵. In contrast, Zn: 134 pm, 3d¹⁰ 4s² has the highest ionization energy among the transitional metals of the same period, and Zn^{2+} , with the electronic configuration 3d¹⁰, is a predominant ion in biological systems. Nature exploits the low oxidation energy of transition metals to facilitate biochemical reactions that involve electron transfer or the reduction of molecules in processes such as the deactivation of reactive oxygen species (ROS) and mitochondrial energy production. Proteins interact with transitional metal by so-called coordination, in which acidic amino acids form non-covalent interactions with the ions of transition metals, thereby creating stable structures

such as heme in hemoglobin and zinc fingers in zinc finger transcription factors. In general, because Fe^{3+} and Mn^{3+} are much more electrophilic than Zn^{2+} , the former (Fe^{3+} and Mn^{3+}) are readily used as electron acceptors, whereas Zn^{2+} is predominantly used as a coordination metal and rarely as a cofactor. Fe^{3+} is abundant in Earth, and, perhaps consequently, many more enzymes in humans use Fe^{3+} as a coordination metal; however, a few enzymes specifically need Mn^{3+} [1].

To function properly, cells need a particular “just right” combination of trace elements [2]. An excess of Mn^{2+} leads to toxicity due to accumulation in mitochondria ([3] and reference therein), and this is associated with the inhibition of mitochondrial enzymes [4,5] and the overproduction of H_2O_2 by mitochondrial superoxide dismutase [6]. Similarly to Mn^{2+} , Zn^{2+} accumulates in mitochondria [7,8], intracellular vesicles [9], the endoplasmic reticulum and the Golgi [10,11]. Accordingly, exposure to high concentrations of Zn^{2+} overloads its intracellular depo and induces mitochondrial dysfunction and apoptosis [12–14]. In contrast, the exposure of normal cells to low levels of Zn^{2+} may have anti-oxidant and anti-apoptotic effects [15–18].

Low concentrations of Mn and Zn are necessary for normal cellular functions and are needed for proliferation [15], the inhibition [17] or induction of cell death [13], transcriptional regulation [19], ROS homeostasis [6,20,21] and keratinocyte differentiation [22], among others. To maintain and regulate Mn and Zn concentrations, multiple mechanisms are in place, including ion exchangers [23,24]; metallothioneins and glutathione buffering systems [25]; and the concentration of ions into vesicles, which can be transported out of cells [9,26,27].

Alterations in Mn and Zn homeostasis are associated with pathological conditions, such as cardiovascular diseases [28,29], neurodegenerative disorders [30] and autism spectrum disorders [31,32]. Recently, it became evident that alterations in Zn and Mn might be a factor that impacts cancerogenesis, e.g., in prostate cancer [33,34], colorectal cancer [35,36], lung cancers [37] and glioblastoma [38], among others [39]. Mutations and the altered expression of ion carriers that regulate Zn and Mn homeostasis are hallmarks of many cancers [40–42]. Intriguingly, cancers often exhibit coordinated changes in Zn^{2+} and Mn^{2+} ion carriers [40,43], although the way in which this modulates ion homeostasis or promotes cancer growth is yet to be investigated. In addition, the modulations of Mn and Zn influence the effectiveness of cancer therapeutics, and several clinical trials are currently underway [13,44–46] (clinical trial.gov NCT03991559, NCT04488783). Here, we discuss the mechanisms of the Zn- and Mn-mediated interactions that influence cancer metabolism related to new diagnostics and therapeutic applications [47–49].

2. Regulation of Zn/Mn Homeostasis

As discussed in the Introduction, alterations in Mn and Zn concentrations influence cell viability. Now, we want to discuss in more detail how Mn- and Zn-based regulation is built. To address this question, we need to analyze a few effects related to Mn and Zn homeostasis. First—what is the intracellular distribution of Mn and Zn, what is the range of the free and protein-bound concentrations of these ions in cells, and how are these concentrations regulated? Second—what is known about the biophysical mechanisms of Mn- and Zn-regulated biological activities inside cells, such as the affinities of proteins to Mn or Zn and reaction constants. Finally, what is known about the influences of Mn and Zn on the biological processes related to cancerogenesis?

2.1. Zn, Mn and ROS Detoxification Reactions

Importantly, Zn^{2+} and Mn^{2+} can catalyze the reduction of superoxide to H_2O_2 by superoxide dismutase, Cu/Zn-SOD1 in the cytoplasm and Mn-SOD2 in mitochondria [50], representing a major route of detoxification in cells (Figure 1) [2,6,51].

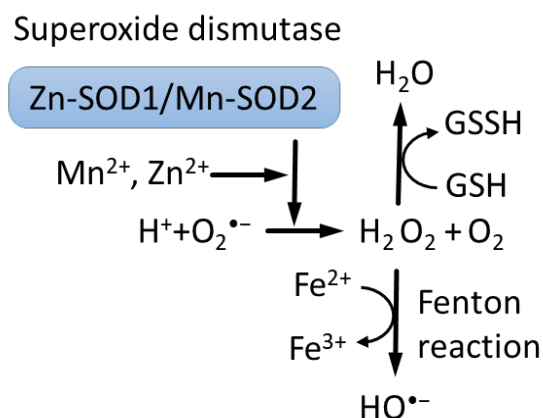


Figure 1. Superoxide dismutases (SODs) use ions of Cu^{2+} or Zn^{2+} and Fe^{3+} or Mn^{2+} to catalyze reduction of superoxide $\text{O}_2^{\bullet-}$ to hydrogen peroxide H_2O_2 [6,52]. In turn, Fenton reaction converts hydrogen peroxide to hydroxyl $\bullet\text{OH}$ radical and hydroxide OH^- ions [53]. Moreover, hydrogen peroxide is converted into water by reduced glutathione (GSH), peroxiredoxins and catalase.

One important difference between Mn^{2+} and Fe^{2+} is that Fe^{2+} catalyzes the Fenton reaction, producing free radical HO^{\bullet} [54,55], whereas Mn^{2+} does not. Thus, Mn^{2+} competition with Fe^{2+} can provide protection, in part, from oxidation-induced degradation [56]. However, mitochondria contain about $16\mu\text{M}$ of free Fe^{2+} , which can participate in the Fenton reaction, promoting the toxicity of Mn^{2+} -driven H_2O_2 overproduction in mitochondria, although this mechanism is debated [6,53,57,58]. It was recently discovered that the concentration of low-molecular-weight complexes of Mn^{2+} with orthophosphates or peptides is a dominant factor that predicts survival and that double-strand breaks repair efficiency after gamma irradiation across bacteria, fungi, archaea and human cells [59].

2.2. Cellular Distribution of Mn and Toxicity

A number of methods for the measurement of intracellular Mn concentrations have been reported in the literature. Interestingly, the addition of Mn to media leads to an increase in Mn concentration in the cell, in some reports way above concentrations in the media, suggesting active transport inside cells [6,60–63]. Using inductively coupled plasma-mass spectrometry, it was shown that the intracellular total Mn concentration in unexposed prostate cancer cells is about $1\mu\text{M}$ and increases upon incubation with 1mM of Mn for 48 h in PC3 ($38.2 \pm 14.3\mu\text{M}$), LNCaP ($34.6 \pm 0.7\mu\text{M}$) and DU145 cells ($12.2 \pm 0.4\mu\text{M}$) [60]. According to measurements using energy-dispersive X-ray fluorescence [61], the total Mn concentration in chick microglia was $45\mu\text{M}$ in the presence of $0.4\mu\text{M}$ of Mn and increased up to $100\mu\text{M}$ with the addition of $2\mu\text{M}$ of Mn. Measurements of Mn in blood cells using graphite-furnace atomic-absorption spectrophotometry with Zeeman background correction revealed an Mn concentration equal to $0.3\mu\text{M}$ in erythrocytes, $0.006\mu\text{M}$ in polymorphonuclear and mononuclear leukocytes, and $0.016\mu\text{M}$ in plasma [64].

It was shown that, upon exposure, Mn^{2+} accumulates mostly in mitochondria [3]; however, Mn^{2+} also binds DNA with $K_d = 33\mu\text{M}$ [65], and there is also accumulation in the nuclei, mostly in the heterochromatin [66]. Consistent with the mitochondria accumulation of Mn^{2+} upon exposure, isolated mitochondria are capable of sucking off the vast majority of exogenously added Mn^{2+} from media [3].

Currently, there are no indicators that would allow measurements of free Mn in living cells beyond the targeted probe [67]. Several Mn-specific molecules have been identified based on their properties to transfer Mn in or out of cells, thereby allowing the measurement of Mn release in media after the pre-loading of cells; however, it is difficult to interpret whether they are mitochondrial or nuclear Mn^{2+} or free cytoplasmic Mn^{2+} [68]. Because Mn^{2+} accumulates in mitochondria upon exposure [3], it is possible to speculate that the free Mn^{2+} concentration in uninduced cells is very low. It is not clear if Mn^{2+} can be released

from mitochondria or other Mn^{2+} deposits as it happens with Zn^{2+} in response to oxidative stress [9].

Cells typically tolerate up to 10 μM of Mn, and the addition of 50 μM or more for 24 h is toxic [6,60,62]. Notably, the addition of Mn to human neuroblastoma cells was found to be a dominant factor driving H_2O_2 production by mitochondrial Mn-SOD2 in the range of an extracellular $MnCl_2$ concentration of 1–100 μM [6]. Upon the addition of extracellular Mn, the fraction of cellular Mn in total protein mass increased over the range of $6.4\text{--}50 \times 10^{-6}$, which, according to the authors' estimation, corresponds to normal physiological ($6.4\text{--}36 \times 10^{-6}$) and pathological (50×10^{-6}) ranges. The addition of as little as 1 μM of Mn increased the mitochondrial oxygen consumption rate, H_2O_2 production and SOD2 activity. It was shown that the overexpression of Mn-SOD2 suppresses breast cancer growth in vitro and in xenograft models [69] and that the mimetics of Mn-SOD2 show anti-cancer activity [70], suggesting that Mn, in the context of SOD activation, has anti-cancer effects. In contrast, recent research has demonstrated an increase in Mn-SOD2 in triple-negative breast cancer, leading to increased stemness and invasiveness of breast cancer cells and M2 macrophage invasion [71].

Apparently, a high concentration of Mn^{2+} (400 μM , 24 h) induces cytochrome C release from mitochondria and caspase-8-mediated apoptosis in B cells [2,72]. It was demonstrated that 10–50 μM of Zn prevents Mn-induced cell death, whereas a higher 100 μM concentration of Zn potentiates human Burkitt lymphoma B cell death (Figure 2) [73]. Similar data were obtained in murine photoreceptor cells [74], and the effect of Zn on cell viability is discussed in the following sections.

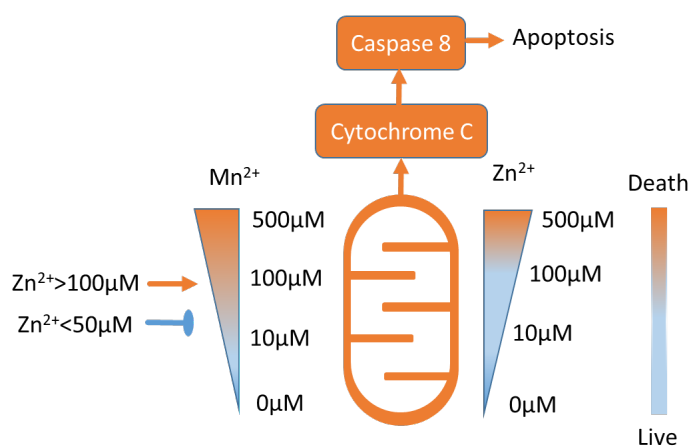


Figure 2. Approximate Mn^{2+} and Zn^{2+} toxicity ranges (see text for details). Low concentrations of Mn^{2+} and Zn^{2+} are not toxic. Notably, Zn^{2+} in concentrations lower than 50 μM inhibits Mn^{2+} -induced toxicity, and Zn^{2+} in concentrations higher than 100 μM potentiates Mn^{2+} toxicity [73].

2.3. Regulation of Zn Homeostasis and Toxicity

In contrast to Mn, it is possible to measure free Zn concentration in cellular organelles using several indicators [11,75–78], and it is generally low, that is, in the order of 5–10 pM in PC12 cells [75] and 400 pM in pancreatic beta cells [76]. Most of the Zn in cells is bound by proteins, and it was estimated that approximately 3000 different proteins in cells bind Zn [79–81]. Among these, metallothionein serves as a major Zn^{2+} buffer, and several other proteins carry the same functions [25,82,83].

Gel filtration chromatography revealed three pools of Zn^{2+} -bound molecules of different molecular weights: metallothionein, other proteins and reduced glutathione (GSH) [84,85]. A comparison of Zn^{2+} affinities for different pools of proteins revealed that apo-metallothionein was able to compete for 13% of Zn^{2+} bound to proteins, GSH competed for 10% of Zn^{2+} and synthetic chelators competed for 32–38% of Zn^{2+} . Thus, the affinity of metallothionein to Zn^{2+} is relatively low in comparison to other Zn proteins; however, due to its abundance, it binds about one-third of cellular Zn^{2+} . Thus, the Zn^{2+} available for protein binding in cells exists in the metallothionein-bound form. Accordingly,

Zn depletion inhibits the activity of transcription factors, and supplementation with free Zn²⁺ or Zn²⁺ in the complex with metallothionein restores it [86,87].

Another one-third of cellular Zn is bound by other non-metallothionein proteins, and the rest of Zn is in the complex with glutathione [84,85,88,89]. It was also shown that the addition of GSH increases the speed of Zn²⁺ binding to proteins other than metallothionein [85,88].

Zn indicators can measure the intracellular distribution of Zn²⁺ [10], and it was revealed that, upon moderate exposure, Zn²⁺ is transferred by TRPM7 (transient receptor potential cation channel subfamily M member 7) into specific vesicles that release Zn²⁺ in response to oxidative stress [9] or in response to TRPM7 agonists, promoting melanoma cell death by inhibiting autophagy [13,90].

Upon exposure to high Zn²⁺ concentrations, cells efflux Zn²⁺ by lysosomal exocytosis [26] and accumulate Zn in mitochondria [7,8], where cell death is then induced [12,14]. The addition of Zn²⁺ to rat primary astrocytes and glioma cells induced GSH depletion, ROS and lactate dehydrogenase induction, mitochondria membrane depolarization and apoptosis [89]. The addition of Zn²⁺ or metallothionein as a Zn²⁺ or Cd²⁺ carrier inhibits membrane potential, ATP production and oxygen consumption by mitochondria [14,91–94].

2.4. Zn and Mn Transport

The transport and distribution of zinc and manganese within cells are regulated by specialized transport proteins (Table 1 and Figure 3). They are conditionally divided into families of Zn importers ZIP/SLC39 and Zn exporters ZNT/SLC30 [11,43].

Table 1. Representative Mn²⁺ and Zn²⁺ ion carrier genes.

Gene Name	Protein Name	Specificity	Type of Transport	Reference
SLC30A10	ZNT10	Mn ²⁺ /Ca ²⁺ exchange, Zn ²⁺ vesicular transport as SLC30A3 heterodimer	Exporter	[95,96]
SLC30A3	ZNT3	Zn ²⁺	Exporter	[39,97–99]
SLC39A14	ZIP14	Divalent metal cations Mn ²⁺ , Zn ²⁺ , Fe ²⁺	Importer (symport)	[97,100–102]
SLC39A8	ZIP8	Mn, Zn, Fe	Importer (symport)	[97,100,103]
TP2C1		Ca or Mn	Mitochondrial influx	[104]

First of all, known Zn exporters use the proton gradient to transfer Zn²⁺ [105]; in contrast, the active transport of Mn²⁺ mediated by SLC30A10 is powered by the import of Ca²⁺ along the electrochemical gradient in exchange to Mn²⁺ across the electrochemical gradient [96]. Moreover, SLC30A10 is capable of transferring Mn²⁺ but not Zn²⁺ [96,106]. In contrast, SLC30A10, as a SLC30A3-SLC30A10 heterodimer, can transport Zn²⁺ and Mn²⁺ into endosomes and activate EGFR/MEK/ERK1,2 transduction, which were found to be reduced by the Zn²⁺ chelator TPEN [107]. In contrast to data from Levi [96], Zhao demonstrated that SLC30A10 overexpression influences Zn²⁺ transport [107].

After Mn²⁺ overexposure, WIF-B human/rat hybrid hepatocytes uptake Mn²⁺ from the cytoplasm by SLC30A10 into vesicles that fuse with the apical cell membrane and release their content in media [108]. Recent data suggest that, similarly to Zn²⁺ [26], Mn²⁺ is released from cancer cells by extracellular vesicles [27].

While SLC30A10 transports Ca²⁺ and Mn²⁺ in opposite directions, ATP2C1 transports Ca²⁺ or Mn²⁺ in the Golgi, preventing Mn²⁺-induced neurotoxicity [104]. The way in which Ca²⁺ entry in cells mediated by SLC30A10 influences Zn-regulated cellular physiology has not been investigated to date. Noticeably, Ca²⁺ entry in monocytes generates free cytoplasmic Zn²⁺ originating in the nuclear and perinuclear endoplasmic reticulum regions [109] or in the mitochondria in neurons [7].

The induction of Zn²⁺ release seems to be required for and precedes ROS generation in mitochondria in response to hypoxia [21,110]. It was reported that Hif1a activation is required for the induction of SLC30A10 expression upon Mn²⁺ exposure [111]. Hif1a is

induced by hypoxia and ROS, and it would be interesting to investigate if SLC30A10 is induced in cancers by similar mechanisms [40].

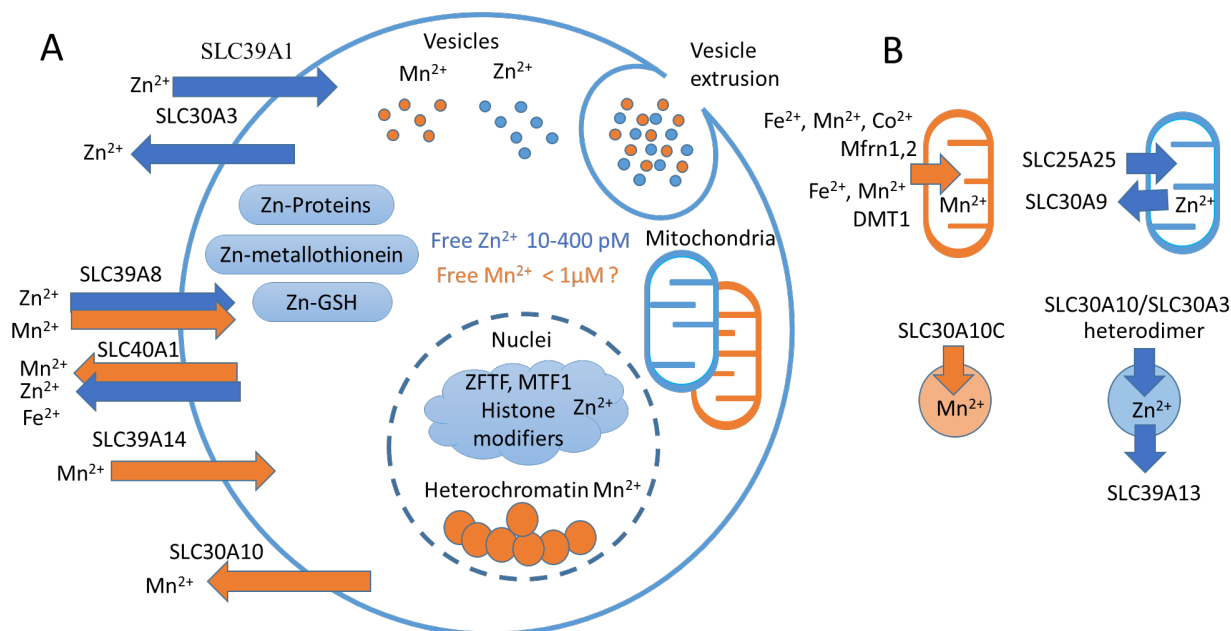


Figure 3. Mn²⁺ and Zn²⁺ homeostasis. (A) Representative scheme of Mn²⁺ and Zn²⁺ transport and cellular compartments. Blue arrows represent Zn²⁺-transporting carriers (SLC39A1, SLC30A3), orange arrows represent Mn²⁺-transporting carriers (SLC39A14, SLC30A10). Double arrows represent proteins that transfer both Mn²⁺ and Zn²⁺ (SLC39A8, SLC40A1). In the cell, Zn²⁺ is distributed between metallothioneins, other proteins and GSH [84,85]. In the nuclei, Zn²⁺ binds MTF1 [25] and serves as a coordination metal for the majority of histone-modifying enzymes [112,113] and zinc finger transcription factors (ZFTFs) [114]. In turn, Mn²⁺ accumulates in heterochromatin [66]. Both Mn²⁺ and Zn²⁺ can accumulate in mitochondria [3,8], as well as in the Golgi apparatus and endoplasmic reticulum [10,11,115,116] (not shown). Both Mn²⁺ and Zn²⁺ can be sequestered in specific vesicles that can be released from the cell [9,26,27]. (B) Ion carriers transfer Mn²⁺ in mitochondria using Mfrn1 [117] and DMT1 [118], and in cellular vesicles by SLC30A10 [108]. In turn, Zn²⁺ is accumulated in mitochondria by SLC25A25 and exerted by SLC30A9 [8,23]. In vesicles, Zn²⁺ is accumulated by SLC30A3-SLC30A10 heterodimer [107] and exerted by SLC39A13 [119].

2.5. Zn and Mn Transporters and Cancerogenesis

The major insights into the functions of zinc transporters in cancerogenesis come from cancer genetics studies [39,120]. In short, the majority of these studies demonstrated reduced Zn levels in different cancers, as well as the corresponding downregulation of importers and the upregulation of exporters [120].

In prostate cancer, zinc deficiency occurs due to the downregulation of zinc transporters [121], and the treatment of prostate cancer cells with physiological concentrations of Zn induces apoptosis [122]. Specifically, the overexpression of Ras-responsive element-binding protein 1 (RREB1) downstream of the Ras-Raf-MEK-ERK signaling pathway represses SLC39A1 (ZIP1) expression leading to a reduced Zn level [123,124]. Preclinical models support the application of Zn²⁺ ionophore clioquinol in combination with a dopamine agonist for prostate cancer treatment [41,125]. In contrast, RREB1/SLC39A3(ZIP3)/Zn were all found to be downregulated in pancreatic adenocarcinoma [126], and a low Zn level was associated with hyperproliferation in vitro. In ovarian cancer, SLC39A13 (ZIP13) and ZIP5, ZIP10, ZIP12 and ZIP14 overexpression were found to be associated with poor prognosis, and SLC39A13 knockout demonstrated suppression of the malignant phenotype in vitro and in vivo and a higher vesicular zinc level in knockout cells [127]. The expression of 10 members of the SLC30 family was measured in cervical carcinoma and revealed a

gradual induction of the Mn^{2+} effluxer SLC30A10 with an increase in cancer stage; complete depletion of the Zn^{2+} vesicular transporter SLC30A8; and the induction of Zn^{2+} exporters SLC30A1, SLC30A6 and SLC30A7 [40].

In turn, due to the superoxide radical scavenger properties of Mn^{2+} [59], high levels of Mn in cancers are associated with poor survival and low radiosensitivity of tumors, such as for melanoma and glioblastoma, in comparison to classical seminoma, breast cancer and prostate cancer [38]. Mn distribution across tissue sections was measured using mass spectrometry. No such correlation was observed for Zn, Cu and Fe in that study. The scanning of tissue sections from the Lewis lung carcinoma metastasis mice model using a similar approach revealed Mn accumulation in a few foci in the primary tumor or in the tissues of untreated animals, whereas the distribution of Zn was uniform [27]. Intriguingly, a higher Mn concentration was detected in organs from the tumor-bearing mice. In addition, sub-toxic 5 μM levels of Mn^{2+} promote cell migration, and exosomal Mn^{2+} exertion was detected [27]. Whether these high Mn regions in the organs of tumor-bearing mice represent metastasis sites or only Mn accumulation requires further investigation.

In this regard, it was demonstrated that Mn^{2+} is the main substrate for SLC39A14 in vivo using mice studies [128] and in humans [100,129], and it is associated with Mn accumulation in blood and most other organs while depleting in the liver. Accordingly, the decreased expression of SLC39A14 was associated with aggressiveness and the relapse of prostate cancer [130], and alternative splicing of SLC39A14 was associated with colorectal cancer [131,132]. However, some studies have found an increase in both Zn and Mn in colorectal cancer tissue, while others observed only a slight difference in Zn levels in males [133,134].

2.6. Transcriptional Regulation by Zn and Mn

Both Zn^{2+} and Mn^{2+} regulate transcription. In neuronal cells, Mn^{2+} induces apoptosis in PC12 cells facilitated by caspase 3 transcriptional activation triggered by the phosphorylation of zinc finger transcription factor SP-1 [135]. In addition, in PC12 cells, Mn^{2+} potentiates histone deacetylase (HDAC) and represses histone acetyltransferase (HAT) activities, leading to the inhibition of the acetylation of core histones [19], which is consistent with the localization of Mn^{2+} in heterochromatin compartments [66]. The inhibition of HDAC activity was found to attenuate cell death, and the inhibition of HAT was found to potentiate Mn^{2+} -induced cell death, suggesting the role of histone acetylation in Mn-induced dopaminergic neurotoxicity [19].

Zinc can regulate transcription because it is a component of many if not all chromatin remodelers, including HDAC, HAT [112,113] and histone demethylases [136,137]. In contrast to Mn in PC12 cells, both Zn^{2+} and zinc transporter ZIP10 activate HAT in keratinocytes, promoting differentiation and the expression of metallothionein genes [22]. Mechanistically, Zn directly regulates the metal-responsive transcription factor 1 (MTF1)-mediated induction of metallothionein genes, thereby generating more Zn^{2+} storage in response to the increase in Zn^{2+} in the environment [25].

A recent paper reports that HDAC8 activity can be regulated by competition between different ions, specifically, Zn^{2+} and Fe^{2+} [113]. The HDAC8 active site has similar architecture to the arginase Mn^{2+} site, in which a single catalytic Zn^{2+} ion is coordinated by two aspartate residues and a histidine [113,138]. HDAC8 exhibits 10^6 higher affinity to Zn^{2+} than to Fe^{2+} (Zn^{2+} ($K_d = 9$ pM); Fe^{2+} ($K_d = 1.1$ μM)), compensating for the higher Fe^{2+} concentrations in cells and higher catalytic activity of HDAC8 in the presence of Fe^{2+} . In addition, HDAC8 can also bind Mn^{2+} and Cu^{2+} , but a comparison of affinities or catalytic activities was not performed [113,138].

Consistent with the roles of Zn [22] and DNA methylation in keratinocyte differentiation [139,140], DNA methyltransferase 1 activity was found to be induced by the depletion of dermis zinc transporter SLC39A13 (ZIP13), and the effect was reversed by Zn supplementation [141].

Consistent with the high affinity of most of the proteins to Zn, the affinity of the third zinc finger of SP-1 to Zn was characterized by $K_d = 6 \times 10^{-10}$, much higher than that for metallothionein [114]. The activity of the Zn-SP-1 transcription factor was evaluated when cellular zinc was depleted using a series of ligands, including apo-metallothionein, glutathione, EDTA, EGTA and TPEN [84]. Out of these, only cell-permeable TPEN at 30 μM was able to inhibit SP-1 binding to DNA in nuclear extracts after 24 h of treatment and completely inhibit DNA binding in vitro. In contrast, Zn inhibited NF- κ B activity, which could be attenuated by an increased metallothionein level [142]. At the same time, the Zn^{2+} -mediated inhibition of Nf- κ B has a profound effect on cancer progression, inhibiting proliferation and inflammation [143–145].

2.7. Mn- and Zn-Mediated Signal Transduction Pathways

In an attempt to reconstitute the Zn-mediated signaling network, the levels of gene expression in response to Zn^{2+} were measured in human intestinal Caco-2 cells with depleted MTF1 [25]. Interestingly, the majority of Zn^{2+} -regulated genes augmented their response, and only metallothioneins and zinc-effluxing Znt1 were less sensitive to Zn^{2+} in the absence of MTF1. This suggests that effective Zn^{2+} levels in the cells became higher due to the diminished buffering capacity of metallothioneins and the efficiency of Zn^{2+} transport out of the cells. This places MTF1 on the top of the Zn-mediated signaling pathway followed by metallothioneins and other Zn-regulated genes. A mathematical model that describes Zn^{2+} homeostasis in cells has been formulated [85].

Zn is known to regulate cancer-related signaling pathways. External Zn^{2+} activates ERK signaling cascades and Ras [146]. Another investigation demonstrated that serum Zn^{2+} represses proapoptotic p38 and JNK signaling, which are activated by the mutant hRas G12V [147]. Nf1 is a classical Ras repressor [148,149], and Zn^{2+} coordination closes Nf1 domains to repress wild-type Ras-GTPase activity in vitro [150].

There are few publications suggesting that Mn^{2+} induces apoptosis or senescence by p53-dependent mechanisms [151–153]. Interestingly, in neuronal cells, Mn^{2+} -induced toxicity was accompanied by increased p53 and mitochondrial p53 localization, while an increase in ROS and mitochondrial H_2O_2 production was attenuated by p53 inhibitors [151]. Similarly, in colorectal cancer cells, Mn-SOD2 overexpression induces p53-dependent senescence [153]. In addition, Mn^{2+} -induced apoptosis was repressed by the DNp73 isoform of the p53 family member p73 [152,154].

The way in which Mn^{2+} regulates p53 activity is not known. One candidate for such regulation is the p53 activator protein phosphatase PP2C α [155], which is characterized by the apparent Mn^{2+} Michaelis constant, $K_{\text{metal}} = 3.3 \text{ mM}$, far above typical total concentrations in cells, and the substitution of Mg^{2+} with Mn^{2+} was found to decrease the activity of the enzyme by a factor of 30 [156]. In the context of p53-dependent apoptosis, it would be interesting to examine if p53 phosphorylation occurs downstream of PP2C activity and the role of the Mg/Mn ratio in the cells.

Besides the p53 activation discussed above, Mn^{2+} induces apoptosis by caspase-8 activation downstream of p38-MSK1 signaling in human B cells [72]. To conclude, Mn^{2+} and Zn^{2+} affect several signaling pathways (p38 and the regulation of histone acetylation) in opposite directions; however, others affect cells in a similar way, including the induction of p53 by Mn^{2+} , the inhibition of Nf- κ B-induced proliferation [144,145,157] and the induction of keratinocyte differentiation by Zn^{2+} ions (Figure 4).

2.8. Differential Effects of Mn and Zn in Normal and Cancer Cells

It was found that zinc sulfate was not toxic to normal cells at 100 μM or below after four days of cultivation, but it significantly decreased the viability of myelogenous leukemia K562 cancer cells at 40 μM and above [158]. It was demonstrated that zinc sulfate protects normal lymphocytes from H_2O_2 -induced DNA damage and augments H_2O_2 -induced DNA damage in K562 cancer cells [158]. The same effect was demonstrated in a recent study of acute myeloid leukemia cells [159]. Similarly, the application of temozolomide and ZnCl_2 at

100 μm enhanced the treatment efficiency of cells and the xenograft model of glioblastoma and did not affect normal human astrocytes [46]. Clinical trials of Zn supplementation in glioblastoma in parallel to temozolomide treatment are currently ongoing (clinicaltrials.gov NCT04488783). A manganese compound Adpa-Mn was found to preferentially induce autophagy and the death of glioblastoma and other cancer cell lines but not astrocytes or non-malignant cells [160,161].

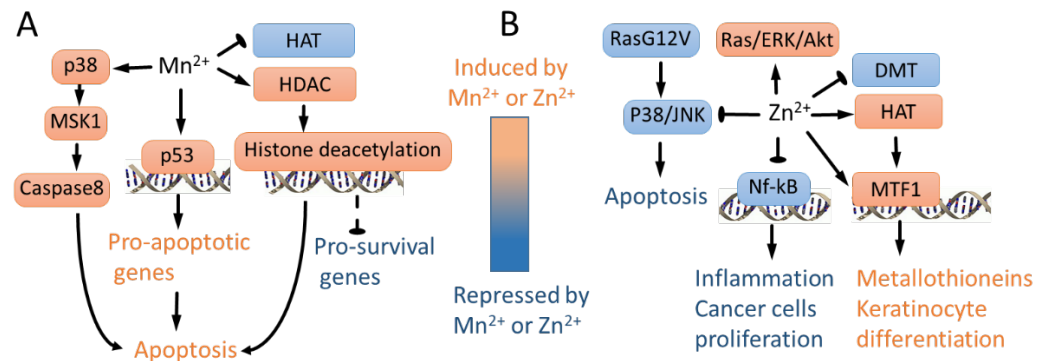


Figure 4. Mn^{2+} - and Zn^{2+} -regulated signaling pathways. (A) Mn^{2+} represses global histone acetylation by augmenting HDAC and repressing HAT activity, leading to apoptosis presumably due to repression of key pro-survival genes [19]. In addition, Mn^{2+} activates p53 [151–153] and p38/MSK1 signaling [72], leading to apoptosis. (B) In wild-type Ras cells, Zn^{2+} activates ERK/AKT signaling [146]. In contrast, in mutant G12V RAS cells, Zn^{2+} inhibits p38 and JNK, repressing apoptosis [147]. Zn^{2+} inhibits Nf- κB , leading to lower proliferation of cancer cells and inhibiting inflammation [144,145,157]. In contrast to Mn^{2+} , Zn^{2+} activates HAT, leading to metallothionein induction and keratinocyte differentiation-specific gene expression [22]. Consistently, Zn^{2+} represses DNA methyltransferase activity in immortalized mouse fibroblasts [141]. Zn directly regulates MTF1-mediated induction of metallothionein genes [25], leading to expression of keratinocyte differentiation genes [22].

3. Effect of Zn and Mn on cGAS-STING Pathway, Immune Response and Cancerogenesis

In addition to coordinately regulating ROS response, transcription and metabolism, Zn^{2+} and Mn^{2+} together regulate a component of the innate immune system, namely, the cGAS-STING (cyclic GMP-AMP synthase—Stimulator of Interferon Genes) pathway, which is activated by cytoplasmic double-stranded DNA caused by viral infection [162] (Figure 5). The cGAS-STING pathway is also involved in the p21-mediated DNA damage response [163] and chromatin stabilization during mitosis upon genotoxic drug treatment [164,165]. cGAS-STING activation requires Mn^{2+} release from intracellular organelles, presumably mitochondria [63]. Mn^{2+} binds to cyclic GMP-AMP synthase (cGAS) and enhances its sensitivity to double-stranded DNA and the production of the secondary messenger cyclic GMP-AMP (cGAMP), leading to Nf κB activation and antiviral response [63,166–169]. It was recently shown that Mn^{2+} is involved in the anti-tumor immune response activated by the cGAS-STING pathway [44]. Mn^{2+} activated both innate and adaptive arms of the immune system, repressed metastasis and potentiated immune checkpoint therapy in mice. A dose-escalating phase 1 clinical trial to estimate the safety and preliminary efficacy of Mn^{2+} -primed anti-PD-1 treatment and chemotherapy is currently ongoing (clinical trial.gov NCT03991559) [44].

In addition, Mn^{2+} potentiates the effect of the TGF- β /PD-L1 bispecific antibody YM101 against several in vivo cancer models by activating the STING pathway and promoting the maturation of mouse and human dendritic cells, shifting the tumor microenvironment toward the inflamed phenotype. This enhances the antigen presentation, infiltration and function of T-lymphocytes [170]. The therapeutic activity of YM101 and Mn^{2+} administration was demonstrated using mice models of hepatocellular carcinoma (H22), melanoma (B16), colon (CT26) cancer and breast (EMT-6) cancers [170]. The application

of self-assembled cyclic dinucleotide STING agonists and Mn^{2+} nanoparticles induced anti-tumor immunity and a remarkable therapeutic effect in multiple tumor models [171].

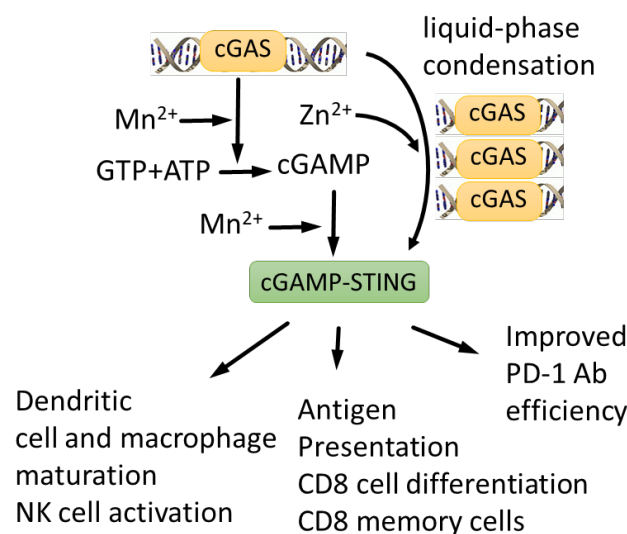


Figure 5. cGAS-STING signaling pathway is activated by both Mn^{2+} and Zn^{2+} . Mn^{2+} is required for efficient DNA sensing, cGAMP synthesis and cGAMP-STING complex formation [63], whereas Zn^{2+} is required for cGAMP folding and liquid-phase separation of cGAMP-DNA complexes [172–174]. Mn^{2+} potentiates cGAS-STING anti-tumor response, stimulating dendritic cell and macrophage maturation, NK cell activation, antigen presentation and CD8 cell differentiation [44]. As a result, Mn^{2+} enhances efficiency of therapeutic antibodies [170].

In turn, Zn^{2+} is also involved in cGAS-STING regulation. Zn^{2+} coordinates the cGAS ribbon, which is essential for the interferon response. Zn^{2+} coordination is also required for cGAS-DNA liquid-phase condensation and cGAMP production [172–174], whereas cGAS binding to DNA is augmented by the zinc finger protein ZCCHC3 [175].

To conclude, recent research supports an anti-cancer role of Zn and Mn via modulation of the inflammatory pathways and immune reactions [44,49,176].

4. Conclusions and Future Perspectives

Transition metal ions Mn^{2+} and Zn^{2+} have profound anti-cancer effects (Table 2). However, their biochemical properties and physiology are different, although with a certain degree of similarity with respect to regulated proteins and metabolic pathways. Taking into account that Mn^{2+} transport proteins also transport Zn^{2+} and other ions, and that a few Mn^{2+} - or Zn^{2+} -specific transporters exist, it is possible to speculate that there are common mechanisms that are regulated by and regulate these ions. Among the few mechanisms commonly influenced by both Mn and Zn are effects on mitochondrial function, including ROS detoxification and the induction of apoptosis, transcriptional regulation and chromatin dynamics, cGAS-STING-mediated apoptosis and the immune response (Table 3).

Many intriguing questions remain to be addressed in future studies. First, conflicting data regarding Zn and Mn concentrations in cancers prompt more detailed studies, in which levels of Zn and Mn in different types of tumor cells should be examined, such as cancer cells and different types of immune and stromal cells from the tumor microenvironment. To address the functions of Mn^{2+} in cell physiology, the field needs to develop intracellular Mn^{2+} probes to be able to monitor the Mn level during investigations in live cells, in a similar fashion to how it is performed for Zn^{2+} . In future experiments, it would be interesting to examine in more detail how Mn^{2+} - and Zn^{2+} -mediated effects are interconnected. For example, cGAS-STING activation is affected by both Zn^{2+} and Mn^{2+} by different mechanisms, and an investigation of the relative impact of these on apoptosis and cancer progression would be interesting.

Table 2. Pivotal findings of Mn²⁺ and Zn²⁺ roles in cancer physiology in vivo.

Main Finding	Reference
Certain cancers exhibit coordinated changes in Zn ²⁺ and Mn ²⁺ carriers	[40,43]
High levels of Mn in cancers are associated with poor survival and low radiosensitivity of tumors, such as for melanoma and glioblastoma	[38]
Preclinical models support application of Zn ²⁺ ionophore clioquinol in combination with dopamine agonist for prostate cancer treatment	[41,125]
Mn ²⁺ boosts innate and adaptive anti-cancer immune response and boosts PD-1 immunotherapy	[44]
Therapeutic activity of YM101 and Mn ²⁺ was demonstrated using mice models of hepatocellular carcinoma, melanoma, colon cancer and breast cancers	[170]
Zn ²⁺ enhances temozolomide efficiency in glioblastoma xenograft model	[46]

Table 3. Pivotal findings of Mn²⁺ and Zn²⁺ roles in cancer physiology in vitro.

Main Finding	References
Mn ²⁺ -SOD2 drives H ₂ O ₂ production in mitochondria in a wide range of extracellular concentrations	[6]
Mn ²⁺ at high concentrations induces mitochondrial cell death	[72,151]
Zn ²⁺ at high concentrations induces mitochondrial cell death	[13,74]
Zn ²⁺ at low concentrations inhibits Mn-induced mitochondrial cell death	[73]
Low-molecular-weight complexes of Mn ²⁺ predict cell survival, and double-strand breaks repair efficiency after gamma irradiation	[59]
Zn ²⁺ release is required for and precedes ROS generation in mitochondria in response to hypoxia	[21,110]
Mn ²⁺ activates p38/MSK1-regulated apoptosis	[72]
Zn ²⁺ inhibits p38 and JNK and represses apoptosis in mutant G12V RAS cells	[147]
Zn ²⁺ activates RAS signaling cascade	[146]
Mn ²⁺ induces apoptosis or senescence by p53-dependent mechanisms	[151–153]
Zn ²⁺ represses NF-κB activity and sensitizes prostate cancer cells to cytotoxic agents	[144,145,157]
Mn ²⁺ represses histone acetylation by repressing HAT activity and augmenting HDAC, leading to apoptosis	[19]
Zn ²⁺ activates HAT and MTF1-mediated transcription, leading to metallothionein induction and keratinocyte differentiation	[22]
Mn ²⁺ is indispensable for cGAS-STNG activation and host defense against DNA viruses	[63]
Zn ²⁺ coordination is required for cGAS–DNA liquid-phase condensation and cGAMP production	[172–174]

We suggest investigations of the combinatorial effects of Zn and Mn on cancers where individual ions have some effect [13,44–46,171]. Recently developed Zn–Mn-composed nanoparticles with potential anti-cancer effects might be useful for such studies [177–180].

Finally, details of such investigations will lead to pre-clinical research and, hopefully, to clinical trials examining the effect of combined Mn and Zn supplementation on the efficiency of anti-cancer drugs.

Author Contributions: J.M.R., M.K., M.S., M.Z., E.K., A.G., A.B., N.B. and K.K. conducted the literature search and wrote this review. All authors have read and agreed to the published version of the manuscript.

Funding: This work was financed by the Russian Scientific Foundation grant 21-74-20066.

Data Availability Statement: Not applicable.

Acknowledgments: This study was made possible through the infrastructural support of the Applied Genetics Resource Facility of MIPT, support 075-15-2021-684.

Conflicts of Interest: Authors M.S. and A.B. were employed by the company OmicsWay Corp. The remaining authors had only academic affiliations. All the authors declare that the research was conducted in the absence of any commercial or financial relationships that could be construed as a potential conflict of interest. The funders had no role in the design of the study; in the collection, analyses, or interpretation of data; in the writing of the manuscript; or in the decision to publish the results.

References

1. Cotruvo, J.A.; Stubbe, J. Metallation and mismetallation of iron and manganese proteins in vitro and in vivo: The class I ribonucleotide reductases as a case study. *Metallomics* **2012**, *4*, 1020–1036. [[CrossRef](#)]
2. Smith, M.R.; Fernandes, J.; Go, Y.-M.; Jones, D.P. Redox dynamics of manganese as a mitochondrial life-death switch. *Biochem. Biophys. Res. Commun.* **2017**, *482*, 388–398. [[CrossRef](#)] [[PubMed](#)]
3. Gunter, T.E.; Gavin, C.E.; Gunter, K.K. The case for manganese interaction with mitochondria. *Neurotoxicology* **2009**, *30*, 727–729. [[CrossRef](#)] [[PubMed](#)]
4. Zheng, W.; Ren, S.; Graziano, J.H. Manganese inhibits mitochondrial aconitase: A mechanism of manganese neurotoxicity. *Brain Res.* **1998**, *799*, 334–342. [[CrossRef](#)]
5. Chen, J.-Y.; Tsao, G.C.; Zhao, Q.; Zheng, W. Differential cytotoxicity of Mn(II) and Mn(III): Special reference to mitochondrial [Fe-S] containing enzymes. *Toxicol. Appl. Pharmacol.* **2001**, *175*, 160–168. [[CrossRef](#)]
6. Fernandes, J.; Hao, L.; Bijli, K.M.; Chandler, J.D.; Orr, M.; Hu, X.; Jones, D.P.; Go, Y.-M. From the Cover: Manganese Stimulates Mitochondrial H₂O₂ Production in SH-SY5Y Human Neuroblastoma Cells over Physiologic as well as Toxicologic Range. *Toxicol. Sci.* **2017**, *155*, 213–223. [[CrossRef](#)]
7. Sensi, S.L.; Ton-That, D.; Weiss, J.H. Mitochondrial sequestration and Ca²⁺-dependent release of cytosolic Zn²⁺ loads in cortical neurons. *Neurobiol. Dis.* **2002**, *10*, 100–108. [[CrossRef](#)]
8. Ma, T.; Zhao, L.; Zhang, J.; Tang, R.; Wang, X.; Liu, N.; Zhang, Q.; Wang, F.; Li, M.; Shan, Q.; et al. A pair of transporters controls mitochondrial Zn²⁺ levels to maintain mitochondrial homeostasis. *Protein Cell* **2022**, *13*, 180–202. [[CrossRef](#)]
9. Abiria, S.A.; Krapivinsky, G.; Sah, R.; Santa-Cruz, A.G.; Chaudhuri, D.; Zhang, J.; Adstamongkonkul, P.; DeCaen, P.G.; Clapham, D.E. TRPM7 senses oxidative stress to release Zn²⁺ from unique intracellular vesicles. *Proc. Natl. Acad. Sci. USA* **2017**, *114*, E6079–E6088. [[CrossRef](#)]
10. Lu, Q.; Haragopal, H.; Slepchenko, K.G.; Stork, C.; Li, Y.V. Intracellular zinc distribution in mitochondria, ER and the Golgi apparatus. *Int. J. Physiol. Pathophysiol. Pharmacol.* **2016**, *8*, 35–43.
11. Chabosseau, P.; Woodier, J.; Cheung, R.; Rutter, G.A. Sensors for measuring subcellular zinc pools. *Metallomics* **2018**, *10*, 229–239. [[CrossRef](#)] [[PubMed](#)]
12. Chen, L.; Yu, X.; Ding, H.; Zhao, Y.; Hu, C.; Feng, J. Comparing the Influence of High Doses of Different Zinc Salts on Oxidative Stress and Energy Depletion in IPEC-J2 Cells. *Biol. Trace Elem. Res.* **2020**, *196*, 481–493. [[CrossRef](#)] [[PubMed](#)]
13. Du, W.; Gu, M.; Hu, M.; Pinchi, P.; Chen, W.; Ryan, M.; Nold, T.; Bannaga, A.; Xu, H. Lysosomal Zn²⁺ release triggers rapid, mitochondria-mediated, non-apoptotic cell death in metastatic melanoma. *Cell Rep.* **2021**, *37*, 109848. [[CrossRef](#)] [[PubMed](#)]
14. Gazaryan, I.G.; Krasinskaya, I.P.; Kristal, B.S.; Brown, A.M. Zinc irreversibly damages major enzymes of energy production and antioxidant defense prior to mitochondrial permeability transition. *J. Biol. Chem.* **2007**, *282*, 24373–24380. [[CrossRef](#)] [[PubMed](#)]
15. Rudolf, E.; Rudolf, K. Increases in Intracellular Zinc Enhance Proliferative Signaling as well as Mitochondrial and Endolysosomal Activity in Human Melanocytes. *Cell. Physiol. Biochem.* **2017**, *43*, 1–16. [[CrossRef](#)] [[PubMed](#)]
16. Prasad, A.S.; Bao, B. Molecular Mechanisms of Zinc as a Pro-Antioxidant Mediator: Clinical Therapeutic Implications. *Antioxidants* **2019**, *8*, 164. [[CrossRef](#)]
17. Wei, Q.; Wang, J.; Wang, M.-H.; Yu, F.; Dong, Z. Inhibition of apoptosis by Zn²⁺ in renal tubular cells following ATP depletion. *Am. J. Physiol. Ren. Physiol.* **2004**, *287*, F492–F500. [[CrossRef](#)]
18. Zhao, Y.; Tan, Y.; Dai, J.; Li, B.; Guo, L.; Cui, J.; Wang, G.; Shi, X.; Zhang, X.; Mellen, N.; et al. Exacerbation of diabetes-induced testicular apoptosis by zinc deficiency is most likely associated with oxidative stress, p38 MAPK activation, and p53 activation in mice. *Toxicol. Lett.* **2011**, *200*, 100–106. [[CrossRef](#)]
19. Guo, Z.; Zhang, Z.; Wang, Q.; Zhang, J.; Wang, L.; Zhang, Q.; Li, H.; Wu, S. Manganese chloride induces histone acetylation changes in neuronal cells: Its role in manganese-induced damage. *Neurotoxicology* **2018**, *65*, 255–263. [[CrossRef](#)]
20. Bonke, E.; Zwicker, K.; Dröse, S. Manganese ions induce H₂O₂ generation at the ubiquinone binding site of mitochondrial complex II. *Arch. Biochem. Biophys.* **2015**, *580*, 75–83. [[CrossRef](#)]
21. Slepchenko, K.G.; Lu, Q.; Li, Y.V. Cross talk between increased intracellular zinc Zn²⁺ and accumulation of reactive oxygen species in chemical ischemia. *Am. J. Physiol. Cell Physiol.* **2017**, *313*, C448–C459. [[CrossRef](#)] [[PubMed](#)]
22. Bin, B.-H.; Lee, S.-H.; Bhin, J.; Irié, T.; Kim, S.; Seo, J.; Mishima, K.; Lee, T.R.; Hwang, D.; Fukada, T.; et al. The epithelial zinc transporter ZIP10 epigenetically regulates human epidermal homeostasis by modulating histone acetyltransferase activity. *Br. J. Dermatol.* **2019**, *180*, 869–880. [[CrossRef](#)] [[PubMed](#)]
23. Deng, H.; Qiao, X.; Xie, T.; Fu, W.; Li, H.; Zhao, Y.; Guo, M.; Feng, Y.; Chen, L.; Zhao, Y.; et al. SLC-30A9 is required for Zn²⁺ homeostasis, Zn²⁺ mobilization, and mitochondrial health. *Proc. Natl. Acad. Sci. USA* **2021**, *118*, e2023909118. [[CrossRef](#)] [[PubMed](#)]
24. Abdo, A.I.; Tran, H.B.; Hodge, S.; Beltrame, J.F.; Zalewski, P.D. Zinc homeostasis alters zinc transporter protein expression in vascular endothelial and smooth muscle cells. *Biol. Trace Elem. Res.* **2021**, *199*, 2158–2171. [[CrossRef](#)]
25. Hardyman, J.E.J.; Tyson, J.; Jackson, K.A.; Aldridge, C.; Cockell, S.J.; Wakeling, L.A.; Valentine, R.A.; Ford, D. Zinc sensing by metal-responsive transcription factor 1 (MTF1) controls metallothionein and ZnT1 expression to buffer the sensitivity of the transcriptome response to zinc. *Metallomics* **2016**, *8*, 337–343. [[CrossRef](#)]
26. Kukic, I.; Kelleher, S.L.; Kiselyov, K. Zn²⁺ efflux through lysosomal exocytosis prevents Zn²⁺-induced toxicity. *J. Cell Sci.* **2014**, *127*, 3094–3103. [[CrossRef](#)]

27. Stelling, M.P.; Soares, M.A.; Cardoso, S.C.; Motta, J.M.; de Abreu, J.C.; Antunes, M.J.M.; de Freitas, V.G.; Moraes, J.A.; Castelo-Branco, M.T.L.; Pérez, C.A.; et al. Manganese systemic distribution is modulated in vivo during tumor progression and affects tumor cell migration and invasion in vitro. *Sci. Rep.* **2021**, *11*, 15833. [[CrossRef](#)]
28. Choi, S.; Liu, X.; Pan, Z. Zinc deficiency and cellular oxidative stress: Prognostic implications in cardiovascular diseases. *Acta Pharmacol. Sin.* **2018**, *39*, 1120–1132. [[CrossRef](#)]
29. Anonna, S.N.; Ahamed, S.K.; Uddin, M.G.; Adnan, M.T.; Uddin, S.M.N.; Hussain, M.S.; Millat, M.S.; Bulbul, L.; Bhatta, R.; Sarwar, M.S.; et al. A clinical evaluation of the alterations in the level of serum zinc, copper, iron, and manganese in the ischemic heart disease patients of Bangladesh—A case-control study. *Heliyon* **2020**, *6*, e05311. [[CrossRef](#)]
30. Mezzaroba, L.; Alfieri, D.F.; Simão, A.N.C.; Reiche, E.M.V. The role of zinc, copper, manganese and iron in neurodegenerative diseases. *Neurotoxicology* **2019**, *74*, 230–241. [[CrossRef](#)]
31. Fiore, M.; Barone, R.; Copat, C.; Grasso, A.; Cristaldi, A.; Rizzo, R.; Ferrante, M. Metal and essential element levels in hair and association with autism severity. *J. Trace Elem. Med. Biol.* **2020**, *57*, 126409. [[CrossRef](#)] [[PubMed](#)]
32. Stanton, J.E.; Malijauskaite, S.; McGourty, K.; Grabrucker, A.M. The metallome as a link between the “omes” in autism spectrum disorders. *Front. Mol. Neurosci.* **2021**, *14*, 695873. [[CrossRef](#)] [[PubMed](#)]
33. Lim, J.T.; Tan, Y.Q.; Valeri, L.; Lee, J.; Geok, P.P.; Chia, S.E.; Ong, C.N.; Seow, W.J. Association between serum heavy metals and prostate cancer risk—A multiple metal analysis. *Environ. Int.* **2019**, *132*, 105109. [[CrossRef](#)] [[PubMed](#)]
34. To, P.K.; Do, M.H.; Cho, J.-H.; Jung, C. Growth modulatory role of zinc in prostate cancer and application to cancer therapeutics. *Int. J. Mol. Sci.* **2020**, *21*, 2991. [[CrossRef](#)] [[PubMed](#)]
35. Nawi, A.M.; Chin, S.-F.; Azhar Shah, S.; Jamal, R. Tissue and Serum Trace Elements Concentration among Colorectal Patients: A Systematic Review of Case-Control Studies. *Iran. J. Public Health* **2019**, *48*, 632–643.
36. Sohrabi, M.; Gholami, A.; Azar, M.H.; Yaghoobi, M.; Shahi, M.M.; Shirmardi, S.; Nikkhah, M.; Kohi, Z.; Salehpour, D.; Khoonsari, M.R.; et al. Trace Element and Heavy Metal Levels in Colorectal Cancer: Comparison between Cancerous and Non-cancerous Tissues. *Biol. Trace Elem. Res.* **2018**, *183*, 1–8. [[CrossRef](#)]
37. Zabłocka-Słowińska, K.; Płaczkowska, S.; Prescha, A.; Pawełczyk, K.; Porębska, I.; Kosacka, M.; Pawlik-Sobecka, L.; Grajeta, H. Serum and whole blood Zn, Cu and Mn profiles and their relation to redox status in lung cancer patients. *J. Trace Elem. Med. Biol.* **2018**, *45*, 78–84. [[CrossRef](#)]
38. Doble, P.A.; Miklos, G.L.G. Distributions of manganese in diverse human cancers provide insights into tumour radioresistance. *Metallomics* **2018**, *10*, 1191–1210. [[CrossRef](#)]
39. Wang, J.; Zhao, H.; Xu, Z.; Cheng, X. Zinc dysregulation in cancers and its potential as a therapeutic target. *Cancer Biol. Med.* **2020**, *17*, 612–625. [[CrossRef](#)]
40. Zhang, J.; Chen, X.-W.; Shu, L.-S.; Liu, C.-D. The correlation and role analysis of SLC30A1 and SLC30A10 in cervical carcinoma. *J. Cancer* **2022**, *13*, 1031–1047. [[CrossRef](#)]
41. Costello, L.C.; Franklin, R.B.; Zou, J.; Naslund, M.J. Evidence that Human Prostate Cancer is a ZIP1-Deficient Malignancy that could be Effectively Treated with a Zinc Ionophore (Clioquinol) Approach. *Chemotherapy* **2015**, *4*, 152. [[CrossRef](#)] [[PubMed](#)]
42. Murali, P.; Johnson, B.P.; Lu, Z.; Climer, L.; Scott, D.A.; Foulquier, F.; Oprea-Ilie, G.; Lupashin, V.; Drake, R.R.; Abbott, K.L. Novel role for the Golgi membrane protein TMEM165 in control of migration and invasion for breast carcinoma. *Oncotarget* **2020**, *11*, 2747–2762. [[CrossRef](#)] [[PubMed](#)]
43. Singh, C.K.; Malas, K.M.; Tydrick, C.; Siddiqui, I.A.; Iczkowski, K.A.; Ahmad, N. Analysis of Zinc-Exporters Expression in Prostate Cancer. *Sci. Rep.* **2016**, *6*, 36772. [[CrossRef](#)] [[PubMed](#)]
44. Lv, M.; Chen, M.; Zhang, R.; Zhang, W.; Wang, C.; Zhang, Y.; Wei, X.; Guan, Y.; Liu, J.; Feng, K.; et al. Manganese is critical for antitumor immune responses via cGAS-STING and improves the efficacy of clinical immunotherapy. *Cell Res.* **2020**, *30*, 966–979. [[CrossRef](#)] [[PubMed](#)]
45. Toren, A.; Yalon, M.; Dafni, A.; Mehrian-Shai, R. Hgg-04. zinc enhances temozolomide cytotoxicity in pediatric glioblastoma multiforme model system. *Neuro-Oncol.* **2020**, *22*, iii344–iii345. [[CrossRef](#)]
46. Toren, A.; Pismenyuk, T.; Yalon, M.; Freedman, S.; Simon, A.J.; Fisher, T.; Moshe, I.; Reichardt, J.K.V.; Constantini, S.; Mardor, Y.; et al. Zinc enhances temozolomide cytotoxicity in glioblastoma multiforme model systems. *Oncotarget* **2016**, *7*, 74860–74871. [[CrossRef](#)]
47. Ekoue, D.N.; He, C.; Diamond, A.M.; Bonini, M.G. Manganese superoxide dismutase and glutathione peroxidase-1 contribute to the rise and fall of mitochondrial reactive oxygen species which drive oncogenesis. *Biochim. Biophys. Acta Bioenerg.* **2017**, *1858*, 628–632. [[CrossRef](#)]
48. Lossow, K.; Schwarz, M.; Kipp, A.P. Are trace element concentrations suitable biomarkers for the diagnosis of cancer? *Redox Biol.* **2021**, *42*, 101900. [[CrossRef](#)]
49. Wang, C.; Zhang, R.; Wei, X.; Lv, M.; Jiang, Z. Metalloimmunology: The metal ion-controlled immunity. *Adv. Immunol.* **2020**, *145*, 187–241. [[CrossRef](#)]
50. Fukai, T.; Ushio-Fukai, M. Superoxide dismutases: Role in redox signaling, vascular function, and diseases. *Antioxid. Redox Signal.* **2011**, *15*, 1583–1606. [[CrossRef](#)]
51. Gordon, S.J.V.; Fenker, D.E.; Vest, K.E.; Padilla-Benavides, T. Manganese influx and expression of ZIP8 is essential in primary myoblasts and contributes to activation of SOD2. *Metallomics* **2019**, *11*, 1140–1153. [[CrossRef](#)] [[PubMed](#)]

52. Azadmanesh, J.; Lutz, W.E.; Coates, L.; Weiss, K.L.; Borgstahl, G.E.O. Direct detection of coupled proton and electron transfers in human manganese superoxide dismutase. *Nat. Commun.* **2021**, *12*, 2079. [[CrossRef](#)] [[PubMed](#)]
53. Thomas, C.; Mackey, M.M.; Diaz, A.A.; Cox, D.P. Hydroxyl radical is produced via the Fenton reaction in submitochondrial particles under oxidative stress: Implications for diseases associated with iron accumulation. *Redox Rep.* **2009**, *14*, 102–108. [[CrossRef](#)] [[PubMed](#)]
54. Gupta, P.; Lakes, A.; Dziubla, T. A free radical primer. In *Oxidative Stress and Biomaterials*; Elsevier: Amsterdam, The Netherlands, 2016; pp. 1–33, ISBN 9780128032695.
55. Henle, E.S.; Luo, Y.; Gassmann, W.; Linn, S. Oxidative damage to DNA constituents by iron-mediated fenton reactions. The deoxyguanosine family. *J. Biol. Chem.* **1996**, *271*, 21177–21186. [[CrossRef](#)] [[PubMed](#)]
56. Smethurst, D.G.J.; Kovalev, N.; McKenzie, E.R.; Pestov, D.G.; Shcherbik, N. Iron-mediated degradation of ribosomes under oxidative stress is attenuated by manganese. *J. Biol. Chem.* **2020**, *295*, 17200–17214. [[CrossRef](#)] [[PubMed](#)]
57. Rauen, U.; Springer, A.; Weisheit, D.; Petrat, F.; Korth, H.-G.; de Groot, H.; Sustmann, R. Assessment of chelatable mitochondrial iron by using mitochondrion-selective fluorescent iron indicators with different iron-binding affinities. *ChemBioChem* **2007**, *8*, 341–352. [[CrossRef](#)]
58. Zsurka, G.; Peeva, V.; Kotlyar, A.; Kunz, W.S. Is There Still Any Role for Oxidative Stress in Mitochondrial DNA-Dependent Aging? *Genes* **2018**, *9*, 175. [[CrossRef](#)]
59. Sharma, A.; Gaidamakova, E.K.; Grichenko, O.; Matrosova, V.Y.; Hoeke, V.; Klimenkova, P.; Conze, I.H.; Volpe, R.P.; Tkavc, R.; Gostinčar, C.; et al. Across the tree of life, radiation resistance is governed by antioxidant Mn^{2+} , gauged by paramagnetic resonance. *Proc. Natl. Acad. Sci. USA* **2017**, *114*, E9253–E9260. [[CrossRef](#)]
60. Hernroth, B.; Holm, I.; Gondikas, A.; Tassidis, H. Manganese inhibits viability of prostate cancer cells. *Anticancer Res.* **2018**, *38*, 137–145. [[CrossRef](#)]
61. Tholey, G.; Ledig, M.; Mandel, P.; Sargentini, L.; Frivold, A.H.; Leroy, M.; Grippo, A.A.; Wedler, F.C. Concentrations of physiologically important metal ions in glial cells cultured from chick cerebral cortex. *Neurochem. Res.* **1988**, *13*, 45–50. [[CrossRef](#)]
62. Liu, Y.; Zhang, R.; Li, P.; Huang, F.; Fa, Z.; Chen, L.; Jiang, X. Determination of the detectable concentration of manganese used in neuronal MEMRI and its effect on cortical neurons in vitro. *Neurol. Res.* **2013**, *35*, 895–902. [[CrossRef](#)] [[PubMed](#)]
63. Wang, C.; Guan, Y.; Lv, M.; Zhang, R.; Guo, Z.; Wei, X.; Du, X.; Yang, J.; Li, T.; Wan, Y.; et al. Manganese Increases the Sensitivity of the cGAS-STING Pathway for Double-Stranded DNA and Is Required for the Host Defense against DNA Viruses. *Immunity* **2018**, *48*, 675–687. [[CrossRef](#)] [[PubMed](#)]
64. Milne, D.B.; Sims, R.L.; Ralston, N.V. Manganese content of the cellular components of blood. *Clin. Chem.* **1990**, *36*, 450–452. [[CrossRef](#)] [[PubMed](#)]
65. Kennedy, S.D.; Bryant, R.G. Manganese-deoxyribonucleic acid binding modes. Nuclear magnetic relaxation dispersion results. *Biophys. J.* **1986**, *50*, 669–676. [[CrossRef](#)]
66. Morello, M.; Canini, A.; Mattioli, P.; Sorge, R.P.; Alimonti, A.; Bocca, B.; Forte, G.; Martorana, A.; Bernardi, G.; Sancesario, G. Sub-cellular localization of manganese in the basal ganglia of normal and manganese-treated rats an electron spectroscopy imaging and electron energy-loss spectroscopy study. *Neurotoxicology* **2008**, *29*, 60–72. [[CrossRef](#)]
67. Bartelle, B.B.; Mana, M.D.; Suero-Abreu, G.A.; Rodriguez, J.J.; Turnbull, D.H. Engineering an effective Mn-binding MRI reporter protein by subcellular targeting. *Magn. Reson. Med.* **2015**, *74*, 1750–1757. [[CrossRef](#)]
68. Kumar, K.K.; Lowe, E.W.; Aboud, A.A.; Neely, M.D.; Redha, R.; Bauer, J.A.; Odak, M.; Weaver, C.D.; Meiler, J.; Aschner, M.; et al. Cellular manganese content is developmentally regulated in human dopaminergic neurons. *Sci. Rep.* **2014**, *4*, 6801. [[CrossRef](#)]
69. Weydert, C.J.; Waugh, T.A.; Ritchie, J.M.; Iyer, K.S.; Smith, J.L.; Li, L.; Spitz, D.R.; Oberley, L.W. Overexpression of manganese or copper-zinc superoxide dismutase inhibits breast cancer growth. *Free Radic. Biol. Med.* **2006**, *41*, 226–237. [[CrossRef](#)]
70. Batinic-Haberle, I.; Tovmasyan, A.; Huang, Z.; Duan, W.; Du, L.; Siamakpour-Reihani, S.; Cao, Z.; Sheng, H.; Spasojevic, I.; Alvarez Secord, A. H_2O_2 -Driven Anticancer Activity of Mn Porphyrins and the Underlying Molecular Pathways. *Oxid. Med. Cell. Longev.* **2021**, *2021*, 6653790. [[CrossRef](#)]
71. Al Haq, A.T.; Tseng, H.-Y.; Chen, L.-M.; Wang, C.-C.; Hsu, H.-L. Targeting prooxidant MnSOD effect inhibits triple-negative breast cancer (TNBC) progression and M2 macrophage functions under the oncogenic stress. *Cell Death Dis.* **2022**, *13*, 49. [[CrossRef](#)]
72. El Mchichi, B.; Hadji, A.; Vazquez, A.; Leca, G. p38 MAPK and MSK1 mediate caspase-8 activation in manganese-induced mitochondria-dependent cell death. *Cell Death Differ.* **2007**, *14*, 1826–1836. [[CrossRef](#)] [[PubMed](#)]
73. Schrantz, N.; Auffredou, M.T.; Bourgeade, M.F.; Besnault, L.; Leca, G.; Vazquez, A. Zinc-mediated regulation of caspases activity: Dose-dependent inhibition or activation of caspase-3 in the human Burkitt lymphoma B cells (Ramos). *Cell Death Differ.* **2001**, *8*, 152–161. [[CrossRef](#)] [[PubMed](#)]
74. Wang, H.; Liu, B.; Yin, X.; Guo, L.; Jiang, W.; Bi, H.; Guo, D. Excessive zinc chloride induces murine photoreceptor cell death via reactive oxygen species and mitochondrial signaling pathway. *J. Inorg. Biochem.* **2018**, *187*, 25–32. [[CrossRef](#)] [[PubMed](#)]
75. Bozym, R.A.; Thompson, R.B.; Stoddard, A.K.; Fierke, C.A. Measuring picomolar intracellular exchangeable zinc in PC-12 cells using a ratiometric fluorescence biosensor. *ACS Chem. Biol.* **2006**, *1*, 103–111. [[CrossRef](#)] [[PubMed](#)]
76. Vinkenborg, J.L.; Nicolson, T.J.; Bellomo, E.A.; Koay, M.S.; Rutter, G.A.; Merckx, M. Genetically encoded FRET sensors to monitor intracellular Zn^{2+} homeostasis. *Nat. Methods* **2009**, *6*, 737–740. [[CrossRef](#)] [[PubMed](#)]
77. Carter, K.P.; Young, A.M.; Palmer, A.E. Fluorescent sensors for measuring metal ions in living systems. *Chem. Rev.* **2014**, *114*, 4564–4601. [[CrossRef](#)]

78. Gee, K.R.; Zhou, Z.-L.; Ton-That, D.; Sensi, S.L.; Weiss, J.H. Measuring zinc in living cells. *Cell Calcium* **2002**, *31*, 245–251. [[CrossRef](#)]
79. Andreini, C.; Banci, L.; Bertini, I.; Rosato, A. Counting the zinc-proteins encoded in the human genome. *J. Proteome Res.* **2006**, *5*, 196–201. [[CrossRef](#)]
80. Tran, J.B.; Krężel, A. InterMetalDB: A Database and Browser of Intermolecular Metal Binding Sites in Macromolecules with Structural Information. *J. Proteome Res.* **2021**, *20*, 1889–1901. [[CrossRef](#)]
81. Ireland, S.M.; Martin, A.C.R. Zincbindpredict-Prediction of Zinc Binding Sites in Proteins. *Molecules* **2021**, *26*, 966. [[CrossRef](#)]
82. Peris-Díaz, M.D.; Guran, R.; Domene, C.; de Los Rios, V.; Zitka, O.; Adam, V.; Krężel, A. An Integrated Mass Spectrometry and Molecular Dynamics Simulations Approach Reveals the Spatial Organization Impact of Metal-Binding Sites on the Stability of Metal-Depleted Metallothionein-2 Species. *J. Am. Chem. Soc.* **2021**, *143*, 16486–16501. [[CrossRef](#)] [[PubMed](#)]
83. Thompson, M.W. Regulation of zinc-dependent enzymes by metal carrier proteins. *Biometals* **2022**, *35*, 187–213. [[CrossRef](#)] [[PubMed](#)]
84. Rana, U.; Kothinti, R.; Meeusen, J.; Tabatabai, N.M.; Krezoski, S.; Petering, D.H. Zinc binding ligands and cellular zinc trafficking: Apo-metallothionein, glutathione, TPEN, proteomic zinc, and Zn-Sp1. *J. Inorg. Biochem.* **2008**, *102*, 489–499. [[CrossRef](#)] [[PubMed](#)]
85. Petering, D.H.; Mahim, A. Proteomic high affinity Zn²⁺ trafficking: Where does metallothionein fit in? *Int. J. Mol. Sci.* **2017**, *18*, 1289. [[CrossRef](#)]
86. Cano-Gauci, D.F.; Sarkar, B. Reversible zinc exchange between metallothionein and the estrogen receptor zinc finger. *FEBS Lett.* **1996**, *386*, 1–4. [[CrossRef](#)]
87. Roesijadi, G.; Bogumil, R.; Vasák, M.; Kägi, J.H. Modulation of DNA binding of a tramtrack zinc finger peptide by the metallothionein-thionein conjugate pair. *J. Biol. Chem.* **1998**, *273*, 17425–17432. [[CrossRef](#)]
88. Mahim, A.; Karim, M.; Petering, D.H. Zinc trafficking 1. Probing the roles of proteome, metallothionein, and glutathione. *Metallomics* **2021**, *13*, mfab055. [[CrossRef](#)]
89. Ryu, R.; Shin, Y.; Choi, J.-W.; Min, W.; Ryu, H.; Choi, C.-R.; Ko, H. Depletion of intracellular glutathione mediates zinc-induced cell death in rat primary astrocytes. *Exp. Brain Res.* **2002**, *143*, 257–263. [[CrossRef](#)]
90. Xing, Y.; Wei, X.; Wang, M.-M.; Liu, Y.; Sui, Z.; Wang, X.; Zhang, Y.; Fei, Y.-H.; Jiang, Y.; Lu, C.; et al. Stimulating TRPM7 suppresses cancer cell proliferation and metastasis by inhibiting autophagy. *Cancer Lett.* **2022**, *525*, 179–197. [[CrossRef](#)]
91. Kukoyi, B.I.; Costello, L.C.; Franklin, R.B. The effect of exogenous zinc ions on the pattern of oxygen consumption of the hepatic mitochondria of albino rats. *Afr. J. Med. Med. Sci.* **2004**, *33*, 361–363.
92. Costello, L.C.; Guan, Z.; Kukoyi, B.; Feng, P.; Franklin, R.B. Terminal oxidation and the effects of zinc in prostate versus liver mitochondria. *Mitochondrion* **2004**, *4*, 331–338. [[CrossRef](#)] [[PubMed](#)]
93. Simpkins, C.; Balderman, S.; Mensah, E. Mitochondrial oxygen consumption is synergistically inhibited by metallothionein and calcium. *J. Surg. Res.* **1998**, *80*, 16–21. [[CrossRef](#)] [[PubMed](#)]
94. Chang, I.; Cho, N.; Koh, J.-Y.; Lee, M.-S. Pyruvate inhibits zinc-mediated pancreatic islet cell death and diabetes. *Diabetologia* **2003**, *46*, 1220–1227. [[CrossRef](#)] [[PubMed](#)]
95. Mercadante, C.J.; Prajapati, M.; Conboy, H.L.; Dash, M.E.; Herrera, C.; Pettiglio, M.A.; Cintron-Rivera, L.; Salesky, M.A.; Rao, D.B.; Bartnikas, T.B. Manganese transporter Slc30a10 controls physiological manganese excretion and toxicity. *J. Clin. Investig.* **2019**, *129*, 5442–5461. [[CrossRef](#)] [[PubMed](#)]
96. Levy, M.; Elkoshi, N.; Barber-Zucker, S.; Hoch, E.; Zarivach, R.; Hershinkel, M.; Sekler, I. Zinc transporter 10 (ZnT10)-dependent extrusion of cellular Mn²⁺ is driven by an active Ca²⁺-coupled exchange. *J. Biol. Chem.* **2019**, *294*, 5879–5889. [[CrossRef](#)]
97. Fujishiro, H.; Kambe, T. Manganese transport in mammals by zinc transporter family proteins, ZNT and ZIP. *J. Pharmacol. Sci.* **2022**, *148*, 125–133. [[CrossRef](#)]
98. Bafaro, E.; Liu, Y.; Xu, Y.; Dempski, R.E. The emerging role of zinc transporters in cellular homeostasis and cancer. *Signal Transduct. Target. Ther.* **2017**, *2*, 17029. [[CrossRef](#)]
99. Huang, L.; Tapaamorndech, S. The SLC30 family of zinc transporters—A review of current understanding of their biological and pathophysiological roles. *Mol. Asp. Med.* **2013**, *34*, 548–560. [[CrossRef](#)]
100. Winslow, J.W.W.; Limesand, K.H.; Zhao, N. The functions of ZIP8, ZIP14, and znt10 in the regulation of systemic manganese homeostasis. *Int. J. Mol. Sci.* **2020**, *21*, 3304. [[CrossRef](#)]
101. Franz, M.-C.; Simonin, A.; Graeter, S.; Hediger, M.A.; Kovacs, G. Development of the First Fluorescence Screening Assay for the SLC39A2 Zinc Transporter. *J. Biomol. Screen.* **2014**, *19*, 909–916. [[CrossRef](#)]
102. Zhao, N.; Zhang, A.-S.; Wortham, A.M.; Jue, S.; Knutson, M.D.; Enns, C.A. The tumor suppressor, P53, decreases the metal transporter, ZIP14. *Nutrients* **2017**, *9*, 1335. [[CrossRef](#)] [[PubMed](#)]
103. Wang, C.-Y.; Jenkitkasemwong, S.; Duarte, S.; Sparkman, B.K.; Shawki, A.; Mackenzie, B.; Knutson, M.D. ZIP8 is an iron and zinc transporter whose cell-surface expression is up-regulated by cellular iron loading. *J. Biol. Chem.* **2012**, *287*, 34032–34043. [[CrossRef](#)] [[PubMed](#)]
104. Mukhopadhyay, S.; Linstedt, A.D. Identification of a gain-of-function mutation in a Golgi P-type ATPase that enhances Mn²⁺ efflux and protects against toxicity. *Proc. Natl. Acad. Sci. USA* **2011**, *108*, 858–863. [[CrossRef](#)]
105. Ohana, E.; Hoch, E.; Keasar, C.; Kambe, T.; Yifrach, O.; Hershinkel, M.; Sekler, I. Identification of the Zn²⁺ binding site and mode of operation of a mammalian Zn²⁺ transporter. *J. Biol. Chem.* **2009**, *284*, 17677–17686. [[CrossRef](#)] [[PubMed](#)]

106. Nishito, Y.; Tsuji, N.; Fujishiro, H.; Takeda, T.-A.; Yamazaki, T.; Teranishi, F.; Okazaki, F.; Matsunaga, A.; Tuschl, K.; Rao, R.; et al. Direct comparison of manganese detoxification/efflux proteins and molecular characterization of znt10 protein as a manganese transporter. *J. Biol. Chem.* **2016**, *291*, 14773–14787. [[CrossRef](#)] [[PubMed](#)]
107. Zhao, Y.; Feresin, R.G.; Falcon-Perez, J.M.; Salazar, G. Differential Targeting of SLC30A10/ZnT10 Heterodimers to Endolysosomal Compartments Modulates EGF-Induced MEK/ERK1/2 Activity. *Traffic* **2016**, *17*, 267–288. [[CrossRef](#)]
108. Thompson, K.J.; Hein, J.; Baez, A.; Sosa, J.C.; Wessling-Resnick, M. Manganese transport and toxicity in polarized WIF-B hepatocytes. *Am. J. Physiol. Gastrointest. Liver Physiol.* **2018**, *315*, G351–G363. [[CrossRef](#)]
109. Yamasaki, S.; Sakata-Sogawa, K.; Hasegawa, A.; Suzuki, T.; Kabu, K.; Sato, E.; Kurosaki, T.; Yamashita, S.; Tokunaga, M.; Nishida, K.; et al. Zinc is a novel intracellular second messenger. *J. Cell Biol.* **2007**, *177*, 637–645. [[CrossRef](#)]
110. Slepchenko, K.G.; Lu, Q.; Li, Y.V. Zinc wave during the treatment of hypoxia is required for initial reactive oxygen species activation in mitochondria. *Int. J. Physiol. Pathophysiol. Pharmacol.* **2016**, *8*, 44–51.
111. Liu, C.; Jursa, T.; Aschner, M.; Smith, D.R.; Mukhopadhyay, S. Up-regulation of the manganese transporter SLC30A10 by hypoxia-inducible factors defines a homeostatic response to manganese toxicity. *Proc. Natl. Acad. Sci. USA* **2021**, *118*, e2107673118. [[CrossRef](#)]
112. Vannini, A.; Volpari, C.; Filocamo, G.; Casavola, E.C.; Brunetti, M.; Renzoni, D.; Chakravarty, P.; Paolini, C.; De Francesco, R.; Gallinari, P.; et al. Crystal structure of a eukaryotic zinc-dependent histone deacetylase, human HDAC8, complexed with a hydroxamic acid inhibitor. *Proc. Natl. Acad. Sci. USA* **2004**, *101*, 15064–15069. [[CrossRef](#)] [[PubMed](#)]
113. Dowling, D.P.; Gattis, S.G.; Fierke, C.A.; Christianson, D.W. Structures of metal-substituted human histone deacetylase 8 provide mechanistic inferences on biological function. *Biochemistry* **2010**, *49*, 5048–5056. [[CrossRef](#)] [[PubMed](#)]
114. Posewitz, M.C.; Wilcox, D.E. Properties of the Sp1 zinc finger 3 peptide: Coordination chemistry, redox reactions, and metal binding competition with metallothionein. *Chem. Res. Toxicol.* **1995**, *8*, 1020–1028. [[CrossRef](#)] [[PubMed](#)]
115. Carmona, A.; Roudeau, S.; Perrin, L.; Veronesi, G.; Ortega, R. Environmental manganese compounds accumulate as Mn(II) within the Golgi apparatus of dopamine cells: Relationship between speciation, subcellular distribution, and cytotoxicity. *Metallomics* **2014**, *6*, 822–832. [[CrossRef](#)]
116. García-Rodríguez, N.; Manzano-López, J.; Muñoz-Bravo, M.; Fernández-García, E.; Muñoz, M.; Wellinger, R.E. Manganese redistribution by calcium-stimulated vesicle trafficking bypasses the need for P-type ATPase function. *J. Biol. Chem.* **2015**, *290*, 9335–9347. [[CrossRef](#)] [[PubMed](#)]
117. Christenson, E.T.; Gallegos, A.S.; Banerjee, A. In vitro reconstitution, functional dissection, and mutational analysis of metal ion transport by mitoferrin-1. *J. Biol. Chem.* **2018**, *293*, 3819–3828. [[CrossRef](#)] [[PubMed](#)]
118. Wolff, N.A.; Garrick, M.D.; Zhao, L.; Garrick, L.M.; Ghio, A.J.; Thévenod, F. A role for divalent metal transporter (DMT1) in mitochondrial uptake of iron and manganese. *Sci. Rep.* **2018**, *8*, 211. [[CrossRef](#)]
119. Jeong, J.; Walker, J.M.; Wang, F.; Park, J.G.; Palmer, A.E.; Giunta, C.; Rohrbach, M.; Steinmann, B.; Eide, D.J. Promotion of vesicular zinc efflux by ZIP13 and its implications for spondylocheiro dysplastic Ehlers-Danlos syndrome. *Proc. Natl. Acad. Sci. USA* **2012**, *109*, E3530–E3538. [[CrossRef](#)]
120. Pan, Z.; Choi, S.; Ouadid-Ahidouch, H.; Yang, J.-M.; Beattie, J.H.; Korichneva, I. Zinc transporters and dysregulated channels in cancers. *Front. Biosci.* **2017**, *22*, 623–643. [[CrossRef](#)]
121. Costello, L.C.; Franklin, R.B.; Feng, P. Mitochondrial function, zinc, and intermediary metabolism relationships in normal prostate and prostate cancer. *Mitochondrion* **2005**, *5*, 143–153. [[CrossRef](#)]
122. Feng, P.; Li, T.-L.; Guan, Z.-X.; Franklin, R.B.; Costello, L.C. Direct effect of zinc on mitochondrial apoptosis in prostate cells. *Prostate* **2002**, *52*, 311–318. [[CrossRef](#)] [[PubMed](#)]
123. Franklin, R.B.; Feng, P.; Milon, B.; Desouki, M.M.; Singh, K.K.; Kajdacsy-Balla, A.; Bagasra, O.; Costello, L.C. hZIP1 zinc uptake transporter down regulation and zinc depletion in prostate cancer. *Mol. Cancer* **2005**, *4*, 32. [[CrossRef](#)] [[PubMed](#)]
124. Milon, B.C.; Agyapong, A.; Bautista, R.; Costello, L.C.; Franklin, R.B. Ras responsive element binding protein-1 (RREB-1) down-regulates hZIP1 expression in prostate cancer cells. *Prostate* **2010**, *70*, 288–296. [[CrossRef](#)] [[PubMed](#)]
125. Costello, L.C.; Franklin, R.B. A Proposed Efficacious Treatment with Clioquinol (Zinc Ionophore) and Cabergoline (Prolactin Dopamine Agonist) for the Treatment of Terminal Androgen-independent Prostate Cancer. Why and How? *J. Clin. Res. Oncol.* **2019**, *2*.
126. Franklin, R.B.; Zou, J.; Costello, L.C. The cytotoxic role of RREB1, ZIP3 zinc transporter, and zinc in human pancreatic adenocarcinoma. *Cancer Biol. Ther.* **2014**, *15*, 1431–1437. [[CrossRef](#)]
127. Cheng, X.; Wang, J.; Liu, C.; Jiang, T.; Yang, N.; Liu, D.; Zhao, H.; Xu, Z. Zinc transporter SLC39A13/ZIP13 facilitates the metastasis of human ovarian cancer cells via activating Src/FAK signaling pathway. *J. Exp. Clin. Cancer Res.* **2021**, *40*, 199. [[CrossRef](#)] [[PubMed](#)]
128. Jenkitkasemwong, S.; Akinyode, A.; Paulus, E.; Weiskirchen, R.; Hojyo, S.; Fukada, T.; Giraldo, G.; Schrier, J.; Garcia, A.; Janus, C.; et al. SLC39A14 deficiency alters manganese homeostasis and excretion resulting in brain manganese accumulation and motor deficits in mice. *Proc. Natl. Acad. Sci. USA* **2018**, *115*, E1769–E1778. [[CrossRef](#)]
129. Himeno, S.; Fujishiro, H. Roles of zinc transporters that control the essentiality and toxicity of manganese and cadmium. *Yakugaku Zasshi* **2021**, *141*, 695–703. [[CrossRef](#)]

130. Xu, X.-M.; Wang, C.-G.; Zhu, Y.-D.; Chen, W.-H.; Shao, S.-L.; Jiang, F.-N.; Liao, Q.-D. Decreased expression of SLC 39A14 is associated with tumor aggressiveness and biochemical recurrence of human prostate cancer. *OncoTargets Ther.* **2016**, *9*, 4197–4205. [[CrossRef](#)]
131. Thorsen, K.; Mansilla, F.; Schepeler, T.; Øster, B.; Rasmussen, M.H.; Dyrskjøt, L.; Karni, R.; Akerman, M.; Krainer, A.R.; Laurberg, S.; et al. Alternative splicing of SLC39A14 in colorectal cancer is regulated by the Wnt pathway. *Mol. Cell. Proteom.* **2011**, *10*, M110.002998. [[CrossRef](#)]
132. Sveen, A.; Bakken, A.C.; Ågesen, T.H.; Lind, G.E.; Nesbakken, A.; Nordgård, O.; Brackmann, S.; Rognum, T.O.; Lothe, R.A.; Skotheim, R.I. The exon-level biomarker SLC39A14 has organ-confined cancer-specificity in colorectal cancer. *Int. J. Cancer* **2012**, *131*, 1479–1485. [[CrossRef](#)] [[PubMed](#)]
133. Lavilla, I.; Costas, M.; Miguel, P.S.; Millos, J.; Bendicho, C. Elemental fingerprinting of tumorous and adjacent non-tumorous tissues from patients with colorectal cancer using ICP-MS, ICP-OES and chemometric analysis. *Biometals* **2009**, *22*, 863–875. [[CrossRef](#)] [[PubMed](#)]
134. Juloski, J.T.; Rakic, A.; Ćuk, V.V.; Ćuk, V.M.; Stefanović, S.; Nikolić, D.; Janković, S.; Trbovich, A.M.; De Luka, S.R. Colorectal cancer and trace elements alteration. *J. Trace Elem. Med. Biol.* **2020**, *59*, 126451. [[CrossRef](#)] [[PubMed](#)]
135. Uchida, A.; Oh-hashii, K.; Kiuchi, K.; Hirata, Y. Manganese regulates caspase-3 gene promoter activity by inducing Sp1 phosphorylation in PC12 cells. *Toxicology* **2012**, *302*, 292–298. [[CrossRef](#)]
136. Brito, S.; Lee, M.-G.; Bin, B.-H.; Lee, J.-S. Zinc and its transporters in epigenetics. *Mol. Cells* **2020**, *43*, 323–330. [[CrossRef](#)]
137. Yusuf, A.P.; Abubakar, M.B.; Malami, I.; Ibrahim, K.G.; Abubakar, B.; Bello, M.B.; Qusty, N.; Elazab, S.T.; Imam, M.U.; Alexiou, A.; et al. Zinc metalloproteins in epigenetics and their crosstalk. *Life* **2021**, *11*, 186. [[CrossRef](#)]
138. Gantt, S.L.; Gattis, S.G.; Fierke, C.A. Catalytic activity and inhibition of human histone deacetylase 8 is dependent on the identity of the active site metal ion. *Biochemistry* **2006**, *45*, 6170–6178. [[CrossRef](#)]
139. Rozenberg, J.M.; Bhattacharya, P.; Chatterjee, R.; Glass, K.; Vinson, C. Combinatorial recruitment of CREB, C/EBP β and c-Jun determines activation of promoters upon keratinocyte differentiation. *PLoS ONE* **2013**, *8*, e78179. Available online: <https://pubmed.ncbi.nlm.nih.gov/24244291/> (accessed on 14 April 2022).
140. Rishi, V.; Bhattacharya, P.; Chatterjee, R.; Rozenberg, J.; Zhao, J.; Glass, K.; Fitzgerald, P.; Vinson, C. CpG methylation of half-CRE sequences creates C/EBP α binding sites that activate some tissue-specific genes. *Proc. Natl. Acad. Sci. USA* **2010**, *107*, 20311–20316. [[CrossRef](#)]
141. Lee, M.-G.; Choi, M.-A.; Chae, S.; Kang, M.-A.; Jo, H.; Baek, J.-M.; In, K.-R.; Park, H.; Heo, H.; Jang, D.; et al. Loss of the dermis zinc transporter ZIP13 promotes the mildness of fibrosarcoma by inhibiting autophagy. *Sci. Rep.* **2019**, *9*, 15042. [[CrossRef](#)]
142. Kim, C.H.; Kim, J.H.; Lee, J.; Ahn, Y.S. Zinc-induced NF- κ B inhibition can be modulated by changes in the intracellular metallothionein level. *Toxicol. Appl. Pharmacol.* **2003**, *190*, 189–196. [[CrossRef](#)]
143. Taniguchi, K.; Karin, M. NF- κ B, inflammation, immunity and cancer: Coming of age. *Nat. Rev. Immunol.* **2018**, *18*, 309–324. [[CrossRef](#)] [[PubMed](#)]
144. Uzzo, R.G.; Leavis, P.; Hatch, W.; Gabai, V.L.; Dulin, N.; Zvartau, N.; Kolenko, V.M. Zinc inhibits nuclear factor- κ B activation and sensitizes prostate cancer cells to cytotoxic agents. *Clin. Cancer Res.* **2002**, *8*, 3579–3583. [[PubMed](#)]
145. Pan, Y.; Huang, J.; Xing, R.; Yin, X.; Cui, J.; Li, W.; Yu, J.; Lu, Y. Metallothionein 2A inhibits NF- κ B pathway activation and predicts clinical outcome segregated with TNM stage in gastric cancer patients following radical resection. *J. Transl. Med.* **2013**, *11*, 173. [[CrossRef](#)] [[PubMed](#)]
146. Anson, K.J.; Corbet, G.A.; Palmer, A.E. Zn²⁺ influx activates ERK and Akt signaling pathways. *Proc. Natl. Acad. Sci. USA* **2021**, *118*, e2015786118. [[CrossRef](#)] [[PubMed](#)]
147. Edamatsu, H. Zinc ions negatively regulate proapoptotic signaling in cells expressing oncogenic mutant Ras. *Biometals* **2022**, *35*, 349–362. [[CrossRef](#)]
148. Kahen, E.J.; Brohl, A.; Yu, D.; Welch, D.; Cubitt, C.L.; Lee, J.K.; Chen, Y.; Yoder, S.J.; Teer, J.K.; Zhang, Y.O.; et al. Neurofibromin level directs RAS pathway signaling and mediates sensitivity to targeted agents in malignant peripheral nerve sheath tumors. *Oncotarget* **2018**, *9*, 22571–22585. [[CrossRef](#)]
149. Kiuru, M.; Busam, K.J. The NF1 gene in tumor syndromes and melanoma. *Lab. Investig.* **2017**, *97*, 146–157. [[CrossRef](#)]
150. Naschberger, A.; Baradaran, R.; Rupp, B.; Carroni, M. The structure of neurofibromin isoform 2 reveals different functional states. *Nature* **2021**, *599*, 315–319. [[CrossRef](#)]
151. Wan, C.; Ma, X.; Shi, S.; Zhao, J.; Nie, X.; Han, J.; Xiao, J.; Wang, X.; Jiang, S.; Jiang, J. Pivotal roles of p53 transcription-dependent and -independent pathways in manganese-induced mitochondrial dysfunction and neuronal apoptosis. *Toxicol. Appl. Pharmacol.* **2014**, *281*, 294–302. [[CrossRef](#)]
152. Kim, D.-S.; Jin, H.; Anantharam, V.; Gordon, R.; Kanthasamy, A.; Kanthasamy, A.G. p73 gene in dopaminergic neurons is highly susceptible to manganese neurotoxicity. *Neurotoxicology* **2017**, *59*, 231–239. [[CrossRef](#)] [[PubMed](#)]
153. Behrend, L.; Mohr, A.; Dick, T.; Zwacka, R.M. Manganese superoxide dismutase induces p53-dependent senescence in colorectal cancer cells. *Mol. Cell. Biol.* **2005**, *25*, 7758–7769. [[CrossRef](#)] [[PubMed](#)]
154. Rozenberg, J.M.; Zvereva, S.; Dalina, A.; Blatov, I.; Zubarev, I.; Luppov, D.; Bessmertnyi, A.; Romanishin, A.; Alsoulaiman, L.; Kumeiko, V.; et al. The p53 family member p73 in the regulation of cell stress response. *Biol. Direct* **2021**, *16*, 23. [[CrossRef](#)] [[PubMed](#)]

155. Ofek, P.; Ben-Meir, D.; Kariv-Inbal, Z.; Oren, M.; Lavi, S. Cell cycle regulation and p53 activation by protein phosphatase 2C alpha. *J. Biol. Chem.* **2003**, *278*, 14299–14305. [[CrossRef](#)] [[PubMed](#)]
156. Tanoue, K.; Miller Jenkins, L.M.; Durell, S.R.; Debnath, S.; Sakai, H.; Tagad, H.D.; Ishida, K.; Appella, E.; Mazur, S.J. Binding of a third metal ion by the human phosphatases PP2C α and Wip1 is required for phosphatase activity. *Biochemistry* **2013**, *52*, 5830–5843. [[CrossRef](#)]
157. Jarosz, M.; Olbert, M.; Wyszogrodzka, G.; Młyniec, K.; Librowski, T. Antioxidant and anti-inflammatory effects of zinc. Zinc-dependent NF- κ B signaling. *Inflammopharmacology* **2017**, *25*, 11–24. [[CrossRef](#)]
158. Sliwinski, T.; Czechowska, A.; Kolodziejczak, M.; Jajte, J.; Wisniewska-Jarosinska, M.; Blasiak, J. Zinc salts differentially modulate DNA damage in normal and cancer cells. *Cell Biol. Int.* **2009**, *33*, 542–547. [[CrossRef](#)]
159. Costa, M.I.; Lapa, B.S.; Jorge, J.; Alves, R.; Carreira, I.M.; Sarmento-Ribeiro, A.B.; Gonçalves, A.C. Zinc prevents DNA damage in normal cells but shows genotoxic and cytotoxic effects in acute myeloid leukemia cells. *Int. J. Mol. Sci.* **2022**, *23*, 2567. [[CrossRef](#)]
160. Geng, J.; Li, J.; Huang, T.; Zhao, K.; Chen, Q.; Guo, W.; Gao, J. A novel manganese complex selectively induces malignant glioma cell death by targeting mitochondria. *Mol. Med. Rep.* **2016**, *14*, 1970–1978. [[CrossRef](#)]
161. Liu, J.; Guo, W.; Li, J.; Li, X.; Geng, J.; Chen, Q.; Gao, J. Tumor-targeting novel manganese complex induces ROS-mediated apoptotic and autophagic cancer cell death. *Int. J. Mol. Med.* **2015**, *35*, 607–616. [[CrossRef](#)]
162. Sun, L.; Wu, J.; Du, F.; Chen, X.; Chen, Z.J. Cyclic GMP-AMP synthase is a cytosolic DNA sensor that activates the type I interferon pathway. *Science* **2013**, *339*, 786–791. [[CrossRef](#)] [[PubMed](#)]
163. Li, C.; Liu, W.; Wang, F.; Hayashi, T.; Mizuno, K.; Hattori, S.; Fujisaki, H.; Ikejima, T. DNA damage-triggered activation of cGAS-STING pathway induces apoptosis in human keratinocyte HaCaT cells. *Mol. Immunol.* **2021**, *131*, 180–190. [[CrossRef](#)] [[PubMed](#)]
164. Flynn, P.J.; Koch, P.D.; Mitchison, T.J. Chromatin bridges, not micronuclei, activate cGAS after drug-induced mitotic errors in human cells. *Proc. Natl. Acad. Sci. USA* **2021**, *118*, e2103585118. [[CrossRef](#)] [[PubMed](#)]
165. Basit, A.; Cho, M.-G.; Kim, E.-Y.; Kwon, D.; Kang, S.-J.; Lee, J.-H. The cGAS/STING/TBK1/IRF3 innate immunity pathway maintains chromosomal stability through regulation of p21 levels. *Exp. Mol. Med.* **2020**, *52*, 643–657. [[CrossRef](#)]
166. Zhao, Z.; Ma, Z.; Wang, B.; Guan, Y.; Su, X.-D.; Jiang, Z. Mn²⁺ Directly Activates cGAS and Structural Analysis Suggests Mn²⁺ Induces a Noncanonical Catalytic Synthesis of 2'3'-cGAMP. *Cell Rep.* **2020**, *32*, 108053. [[CrossRef](#)]
167. Sarhan, J.; Liu, B.C.; Muendlein, H.I.; Weindel, C.G.; Smirnova, I.; Tang, A.Y.; Ilyukha, V.; Sorokin, M.; Buzdin, A.; Fitzgerald, K.A.; et al. Constitutive interferon signaling maintains critical threshold of MLKL expression to license necroptosis. *Cell Death Differ.* **2019**, *26*, 332–347. [[CrossRef](#)]
168. Larkin, B.; Ilyukha, V.; Sorokin, M.; Buzdin, A.; Vannier, E.; Poltorak, A. Cutting edge: Activation of STING in T cells induces type I IFN responses and cell death. *J. Immunol.* **2017**, *199*, 397–402. [[CrossRef](#)]
169. Ram, D.R.; Ilyukha, V.; Volkova, T.; Buzdin, A.; Tai, A.; Smirnova, I.; Poltorak, A. Balance between short and long isoforms of cFLIP regulates Fas-mediated apoptosis in vivo. *Proc. Natl. Acad. Sci. USA* **2016**, *113*, 1606–1611. [[CrossRef](#)]
170. Yi, M.; Niu, M.; Zhang, J.; Li, S.; Zhu, S.; Yan, Y.; Li, N.; Zhou, P.; Chu, Q.; Wu, K. Combine and conquer: Manganese synergizing anti-TGF- β /PD-L1 bispecific antibody YM101 to overcome immunotherapy resistance in non-inflamed cancers. *J. Hematol. Oncol.* **2021**, *14*, 146. [[CrossRef](#)]
171. Sun, X.; Zhang, Y.; Li, J.; Park, K.S.; Han, K.; Zhou, X.; Xu, Y.; Nam, J.; Xu, J.; Shi, X.; et al. Amplifying STING activation by cyclic dinucleotide-manganese particles for local and systemic cancer metalloimmunotherapy. *Nat. Nanotechnol.* **2021**, *16*, 1260–1270. [[CrossRef](#)]
172. Du, M.; Chen, Z.J. DNA-induced liquid phase condensation of cGAS activates innate immune signaling. *Science* **2018**, *361*, 704–709. [[CrossRef](#)] [[PubMed](#)]
173. Xie, W.; Lama, L.; Adura, C.; Tomita, D.; Glickman, J.F.; Tuschl, T.; Patel, D.J. Human cGAS catalytic domain has an additional DNA-binding interface that enhances enzymatic activity and liquid-phase condensation. *Proc. Natl. Acad. Sci. USA* **2019**, *116*, 11946–11955. [[CrossRef](#)] [[PubMed](#)]
174. Kranzusch, P.J.; Lee, A.S.-Y.; Berger, J.M.; Doudna, J.A. Structure of human cGAS reveals a conserved family of second-messenger enzymes in innate immunity. *Cell Rep.* **2013**, *3*, 1362–1368. [[CrossRef](#)] [[PubMed](#)]
175. Lian, H.; Wei, J.; Zang, R.; Ye, W.; Yang, Q.; Zhang, X.-N.; Chen, Y.-D.; Fu, Y.-Z.; Hu, M.-M.; Lei, C.-Q.; et al. ZCCHC3 is a co-sensor of cGAS for dsDNA recognition in innate immune response. *Nat. Commun.* **2018**, *9*, 3349. [[CrossRef](#)] [[PubMed](#)]
176. Skrajnowska, D.; Bobrowska-Korczak, B. Role of Zinc in Immune System and Anti-Cancer Defense Mechanisms. *Nutrients* **2019**, *11*, 2273. [[CrossRef](#)]
177. Li, Y.; Du, L.; Li, F.; Deng, Z.; Zeng, S. Intelligent Nanotransducer for Deep-Tumor Hypoxia Modulation and Enhanced Dual-Photosensitizer Photodynamic Therapy. *ACS Appl. Mater. Interfaces* **2022**, *14*, 14944–14952. [[CrossRef](#)]
178. Wang, Y.; Zou, L.; Qiang, Z.; Jiang, J.; Zhu, Z.; Ren, J. Enhancing Targeted Cancer Treatment by Combining Hyperthermia and Radiotherapy Using Mn-Zn Ferrite Magnetic Nanoparticles. *ACS Biomater. Sci. Eng.* **2020**, *6*, 3550–3562. [[CrossRef](#)]
179. Sun, Y.; Yan, C.; Xie, J.; Yan, D.; Hu, K.; Huang, S.; Liu, J.; Zhang, Y.; Gu, N.; Xiong, F. High-Performance Worm-like Mn-Zn Ferrite Theranostic Nanoagents and the Application on Tumor Theranostics. *ACS Appl. Mater. Interfaces* **2019**, *11*, 29536–29548. [[CrossRef](#)]
180. Dippong, T.; Levei, E.A.; Cadar, O. Recent advances in synthesis and applications of mfe₂o₄ (M = co, cu, mn, ni, zn) nanoparticles. *Nanomaterials* **2021**, *11*, 1560. [[CrossRef](#)]